D5-17266-3 Volume 3 of 3

SSME STRUCTURAL COMPUTER PROGRAM DEVELOPMENT

BOPACE DEMONSTRATION ANALYSIS OF THE SSME THRUST CHAMBER LINER

CONTRACT NAS8-29821

(1-3-50-32679[1F])

JULY 31, 1973

PREPARED BY

BOEING AEROSPACE COMPANY
(A division of The Boeing Company)
STRESS & MATERIALS
HUNTSVILLE, ALABAMA

W. H. ARMSTRONG - PROGRAM MANAGER

A. H. SPRING - PRINCIPAL INVESTIGATOR

PREPARED FOR

NATIONAL AERONAUTICS AND SPACE ADMINISTRATION
GEORGE C. MARSHALL SPACE FLIGHT CENTER
MARSHALL SPACE FLIGHT CENTER, ALABAMA

TABLE OF CONTENTS

LIST OF FIGURES

LIST OF FIGURES (CONTINUED)

1.0 DEFINITION OF DEMONSTRATION PROBLEM

The demonstration problem was defined with two objectives in mind. First, the demonstration problem was designed to exercise the full capabilities of the BOPACE program. Second, thermal and mechanical boundary conditions were used which reflect the emergency power level (EPL) operating condition for the SSME 470K engine at a station just upstream of the thrust chamber throat.

The demonstration problem is summarized as follows:

1. Three cycles at a station 1" upstream of the throat of the SSME 470K engine were analyzed.
2. Each cycle is defined by a start transient, sustained burn and shutdown. Sustained burn will last 500 seconds and the shutdown is defined as in previous SSME analysis (Reference 1).
3. For demonstration purposes, the following was included:
   a. Creep behavior based on Boeing test data for NARLOY-Z;
   b. Estimated cyclic behavior of NARLOY-Z;
   c. Specified variation of z-strain from the inside of the liner to the outside of the structural jacket;
   d. Local tangential slip between the liner and Inconel jacket.

1.1 THRUST CHAMBER GEOMETRY

A typical cross section of the SSME thrust chamber is shown on Figure 1.1-1. It consists of a liner of NARLOY-Z with milled coolant passages.

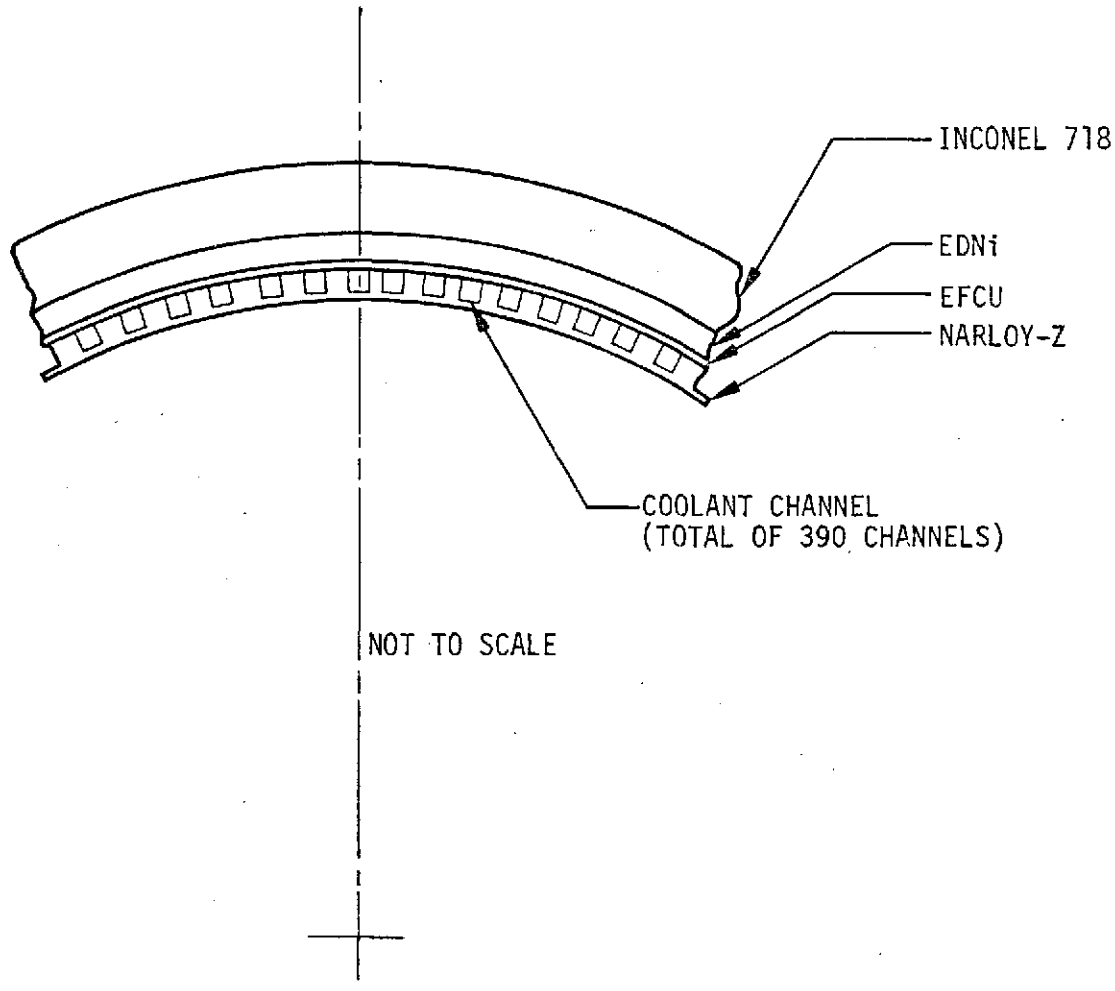

FIGURE 1.1-1: SSME 470K THRUST CHAMBER CROSS SECTION

1.1 (Continued)

The coolant channels are closed out by a layer of electroformed copper (EFCU) and an additional layer of electro-deposited nickel (EDNI). Inconel 718 forms the outer structural shell of the thrust chamber. For the demonstration analysis, a section approximately 25.4 mm (1 inch) upstream of the throat was chosen. Maximum wall temperature occurs at this section.

Symmetry of the channel geometry allows a plane strain analysis of a radial segment of the thrust chamber bounded by radial lines through the centerline of the coolant channel and through the centerline of the land area. Figure 1.1-2 shows the radial segment used in the analysis with the dimensions given for a station 23.85 mm (.939 in.) upstream of the throat.

1.2 EMERGENCY POWER LEVEL CYCLE

The engine cycle consists of a start transient, sustained burn, shutdown and a return to the initial condition. The cycle is characterized by the variation of the hot gas side wall temperature shown in Figure 1.2-1. From an initial condition of 255°K (0°F) the wall temperature remains approximately constant for 1.75 seconds, then rises rapidly to 922°K (1100°F) at 5 seconds. The wall temperature remains at 922°K for 500 seconds (sustained burn), drops to 89°K (-300°F) in approximately 1.4 seconds during shutdown and finally returns to 255°K (0°F)

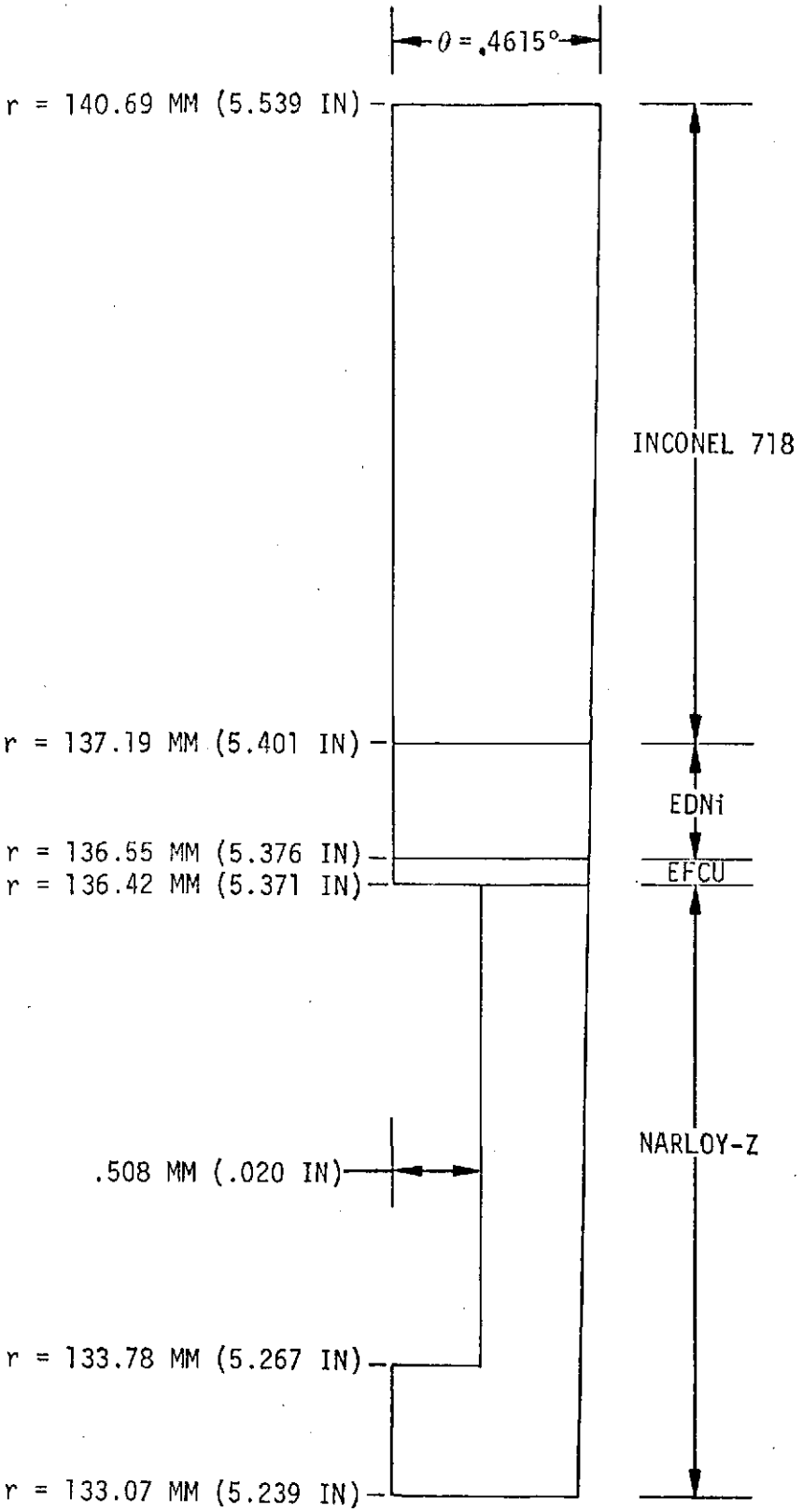

FIGURE 1.1-2: THRUST CHAMBER SEGMENT FOR ANALYSIS

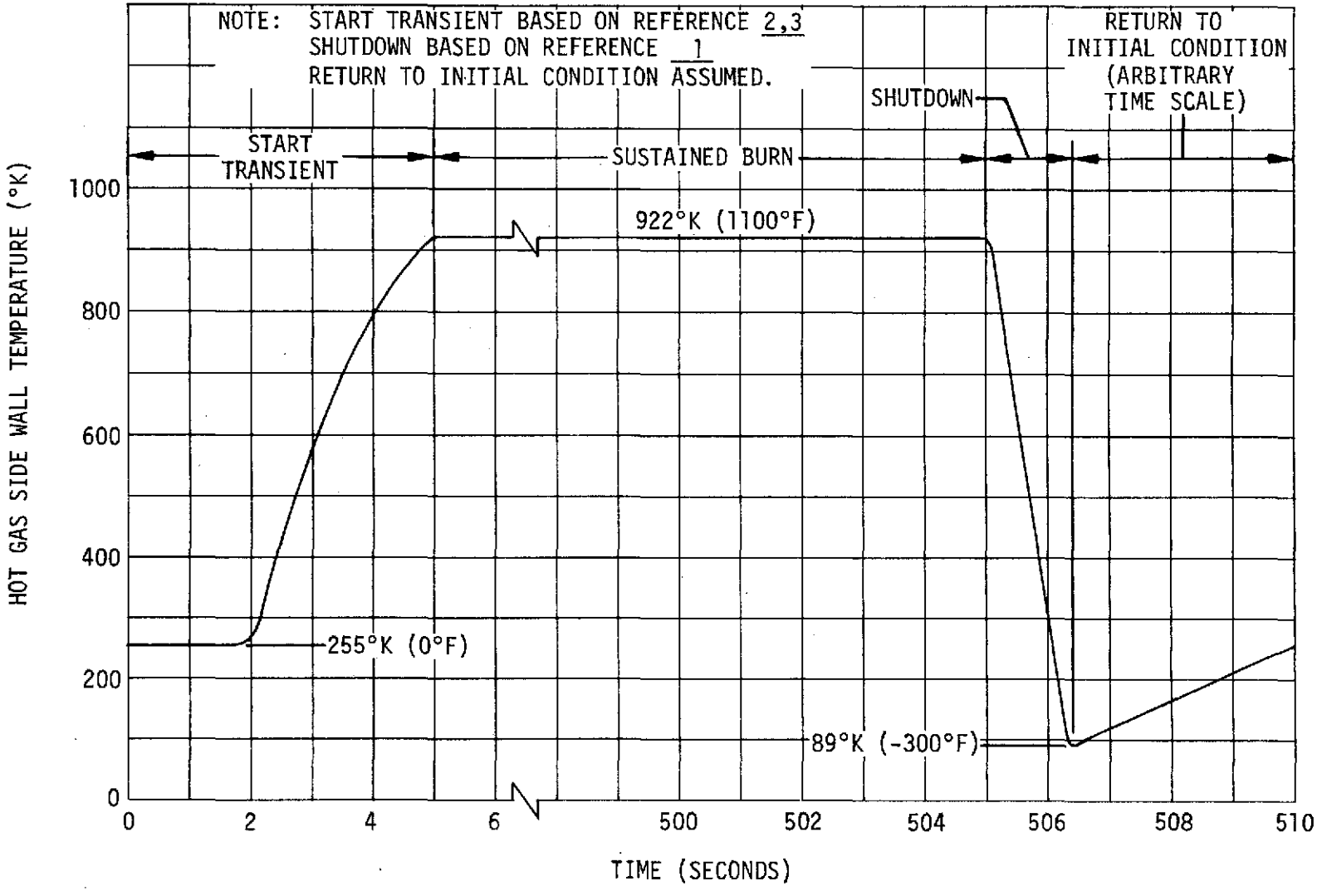

FIGURE 1.2-1: EPL CYCLE IN TERMS OF HOT GAS SIDE WALL TEMPERATURE

1.2 (Continued)

to complete the cycle. Start transient information was obtained from References 2 and 3.

1.3 THERMAL BOUNDARY CONDITIONS

A heat conduction analysis of the engine segment (Figure 1.1-2) was required to determine distributions of temperature over the segment for input to the BOPACE program. The boundary conditions required for the thermal analysis are the hot gas side wall temperature (Figure 1.2-1) and the coolant temperature and flow rate (Figure 1.3-1).

1.4 MECHANICAL BOUNDARY CONDITIONS

The thrust chamber segment analyzed is mechanically loaded by the thrust chamber pressure, the coolant passage pressure, and imposed axial (Z) strains. The time variations of thrust chamber pressure (at the throat) and coolant passage pressure (at the throat) are shown in Figure 1.4-1. The imposed axial strains are assumed to vary linearly from -.1% at the hot gas wall to -.2% at the outside of the jacket. This variation is based on an average -.15% axial strain determined from Rocketdyne stress analysis (Reference 4) and is included to demonstrate BOPACE capability for specified non-zero axial strains.

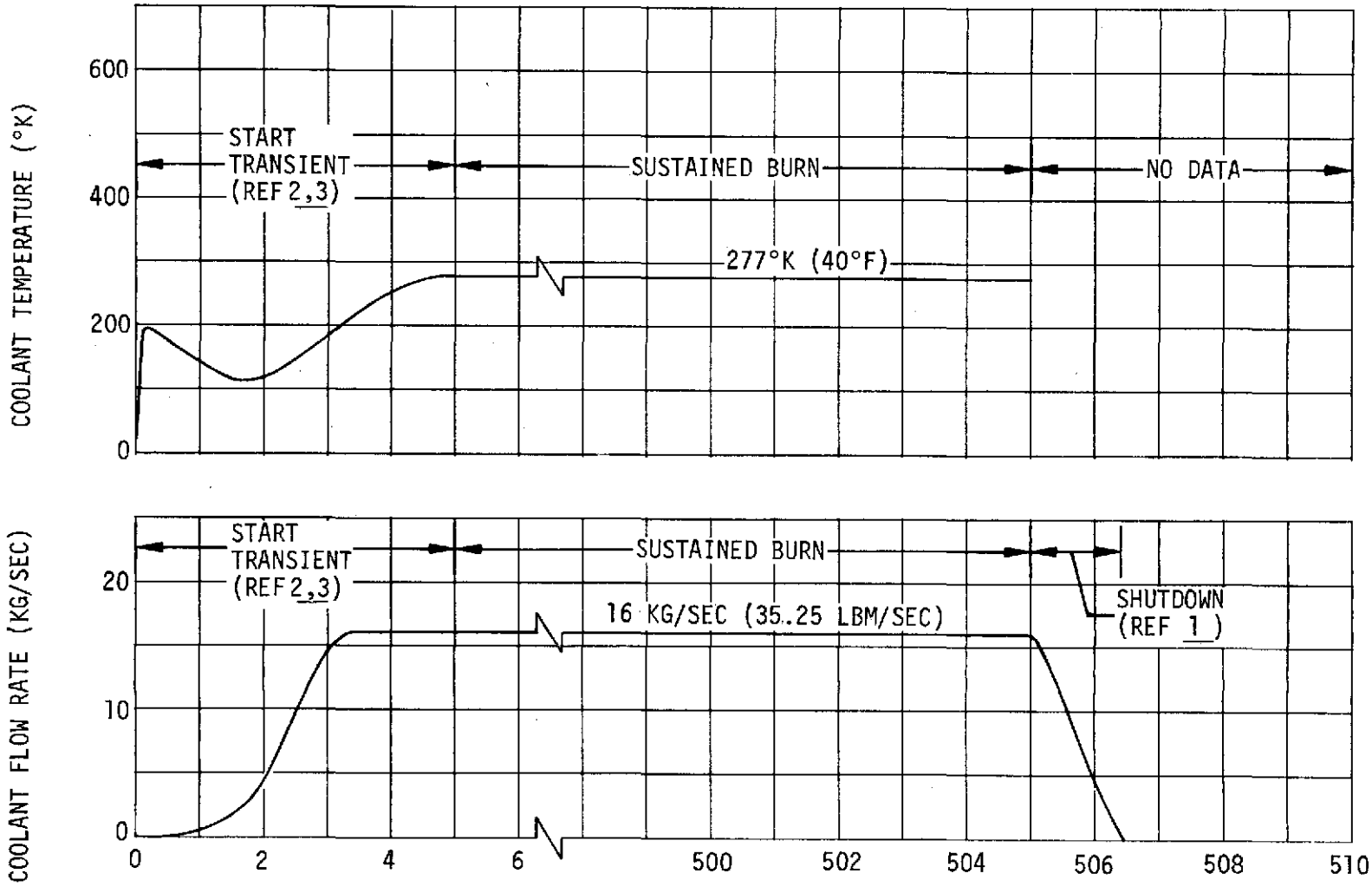

FIGURE 1.3-1: COOLANT TEMPERATURE AND FLOW RATE FOR EPL

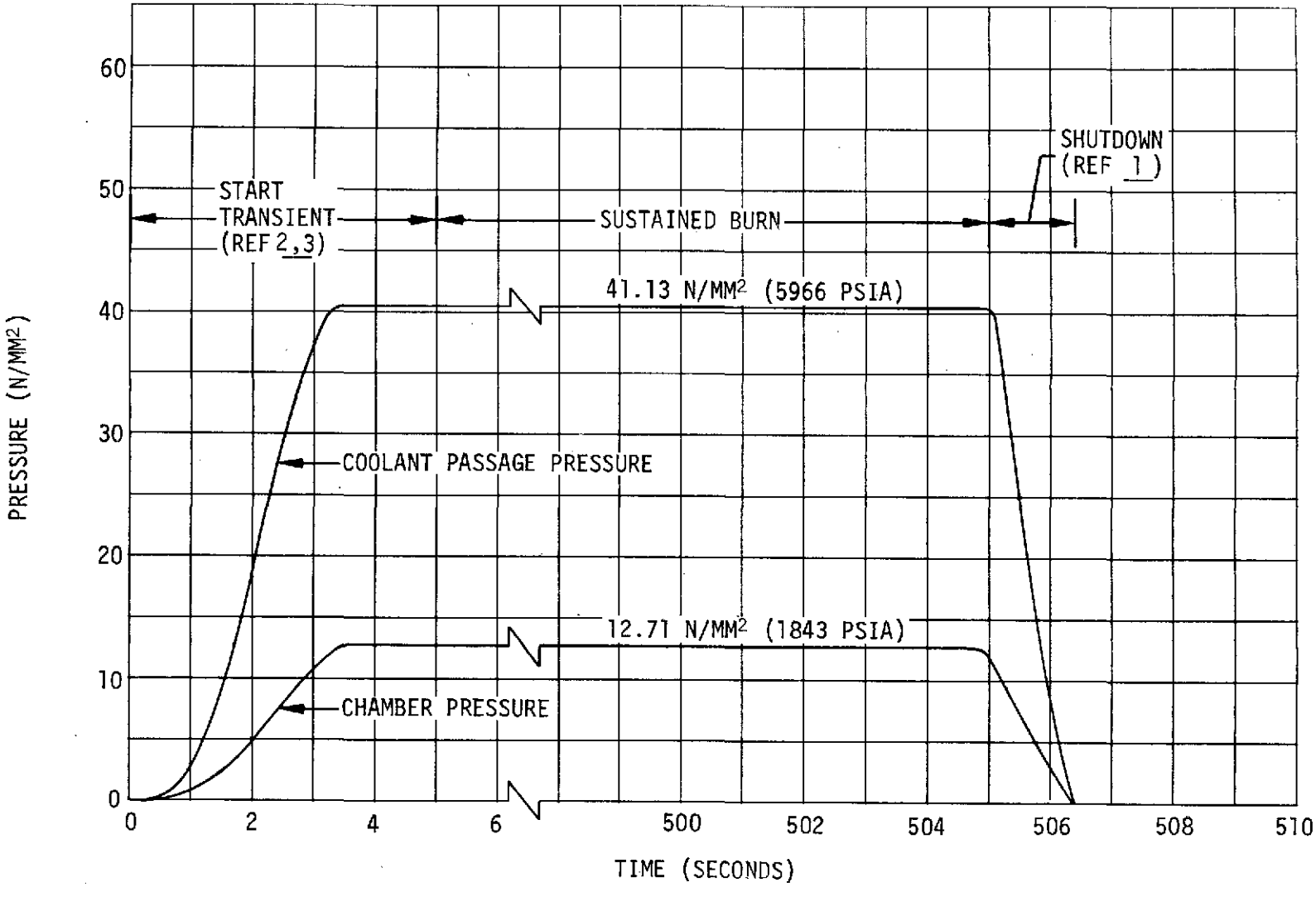

FIGURE 1.4-1: COOLANT PASSAGE AND CHAMBER PRESSURES FOR EPL

1.5 MATERIAL PROPERTIES

Thermal and mechanical properties of the four materials used in the thrust chamber cross section were required as functions of temperature. For the heat conduction analysis, specific heat and thermal conductivity of the four chamber materials were obtained principally from Reference 5.

The mechanical properties required for the analysis are the stress-strain curves, modulus of elasticity, thermal expansion, Poisson's ratio and creep information. These data with the exception of creep information were obtained from Reference 5.

Special consideration was given to the stress-strain curves. For the BOPACE program, stress strain data is represented in terms of a combined hardening theory (Reference 6) which takes account of possible kinematic and isotropic hardening of the material. Plasticity data for the Inconel 718, EDNI and EFCU were assumed to result from kinematic hardening only. As part of the demonstration analysis, the plasticity data for NARLOY-Z were assumed to include isotropic hardening. An isotropic hardening curve (yield surface size versus cumulative plastic strain) was assumed such that a moderate increase in yield point was included. Then curves of kinematic hardening versus plastic strain were developed for an assumed stable condition of the material. The third parameter (kinematic factor versus cumulative plastic strain) were then determined such that the original stress strain data were properly matched. Figures 1.5-1, 1.5-2, and 1.5-3 show these curves for several temperatures.

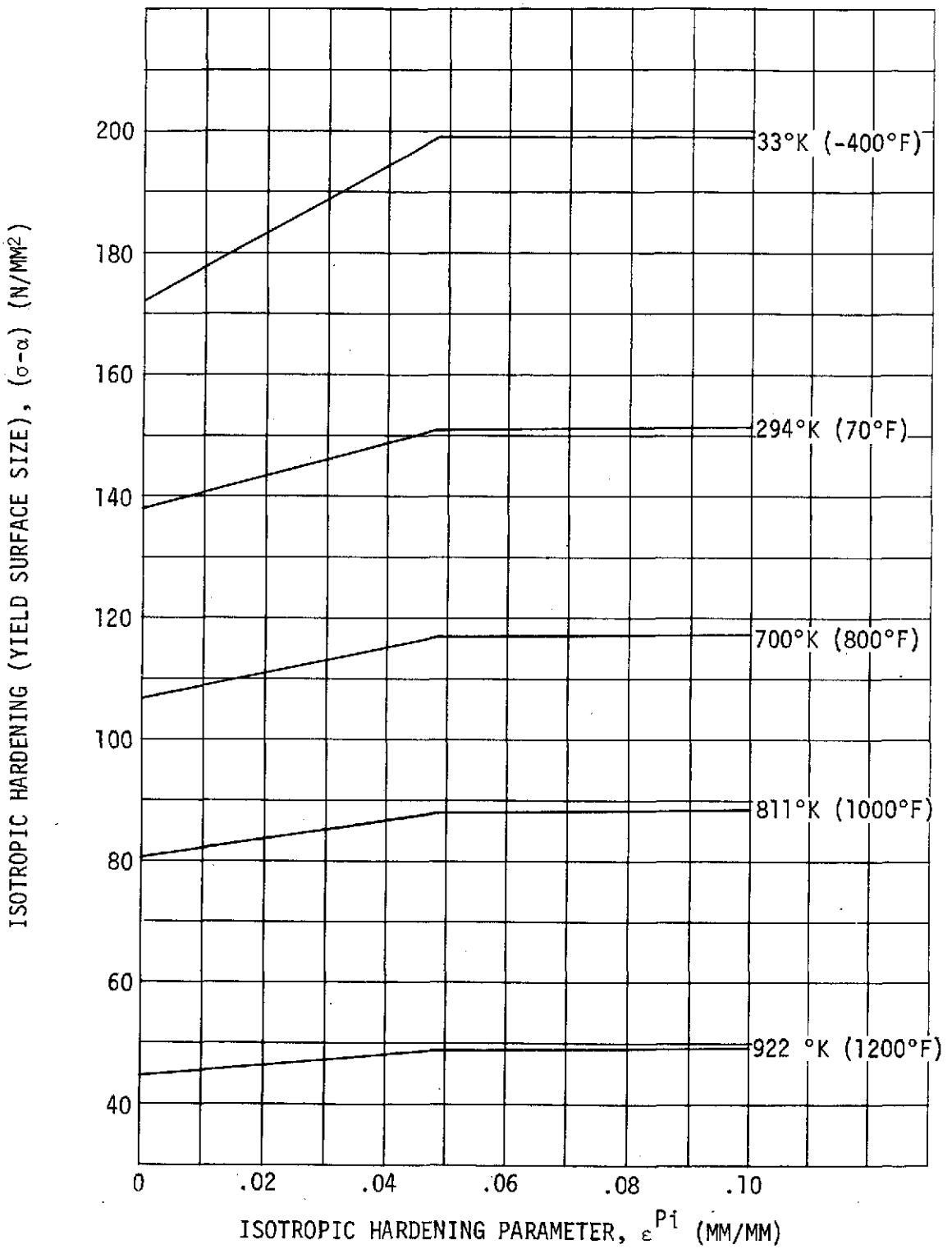

FIGURE 1.5-1: ASSUMED ISOTROPIC HARDENING FOR NARLOY-Z

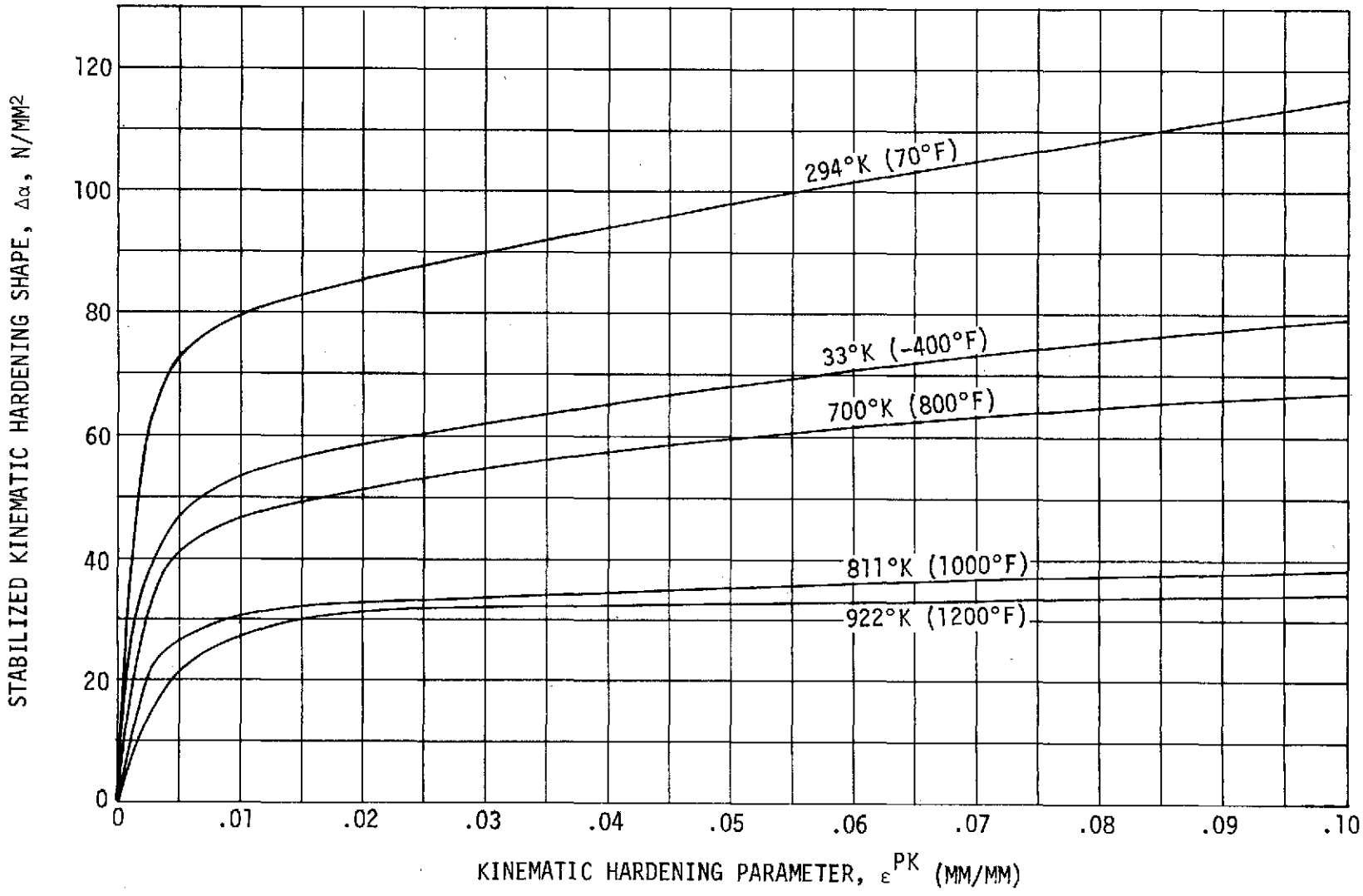

FIGURE 1.5-2: ASSUMED KINEMATIC HARDENING FOR NARLOY-Z

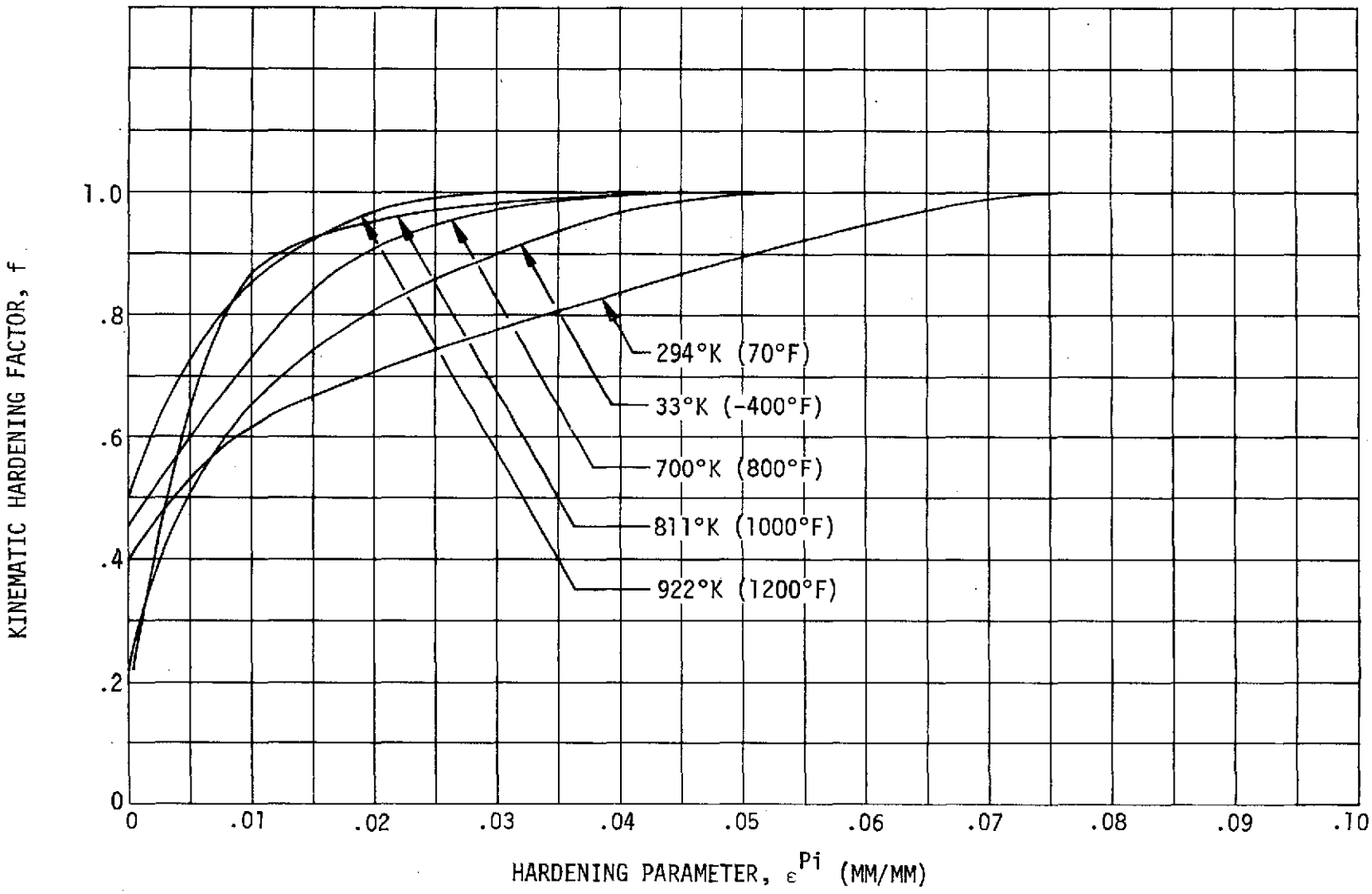

FIGURE 1.5-3: KINEMATIC HARDENING FACTOR FOR NARLOY-Z

1.5 (Continued)

Creep data for NARLOY-Z were included based on preliminary tests (Reference 7). For input to BOPACE, creep information is represented as a reference curve of creep strain versus time (Figure 1.5-4) and a series of curves of creep factor versus stress for various temperatures. The creep factor curves used in this analysis are given in Figure 1.5-5.

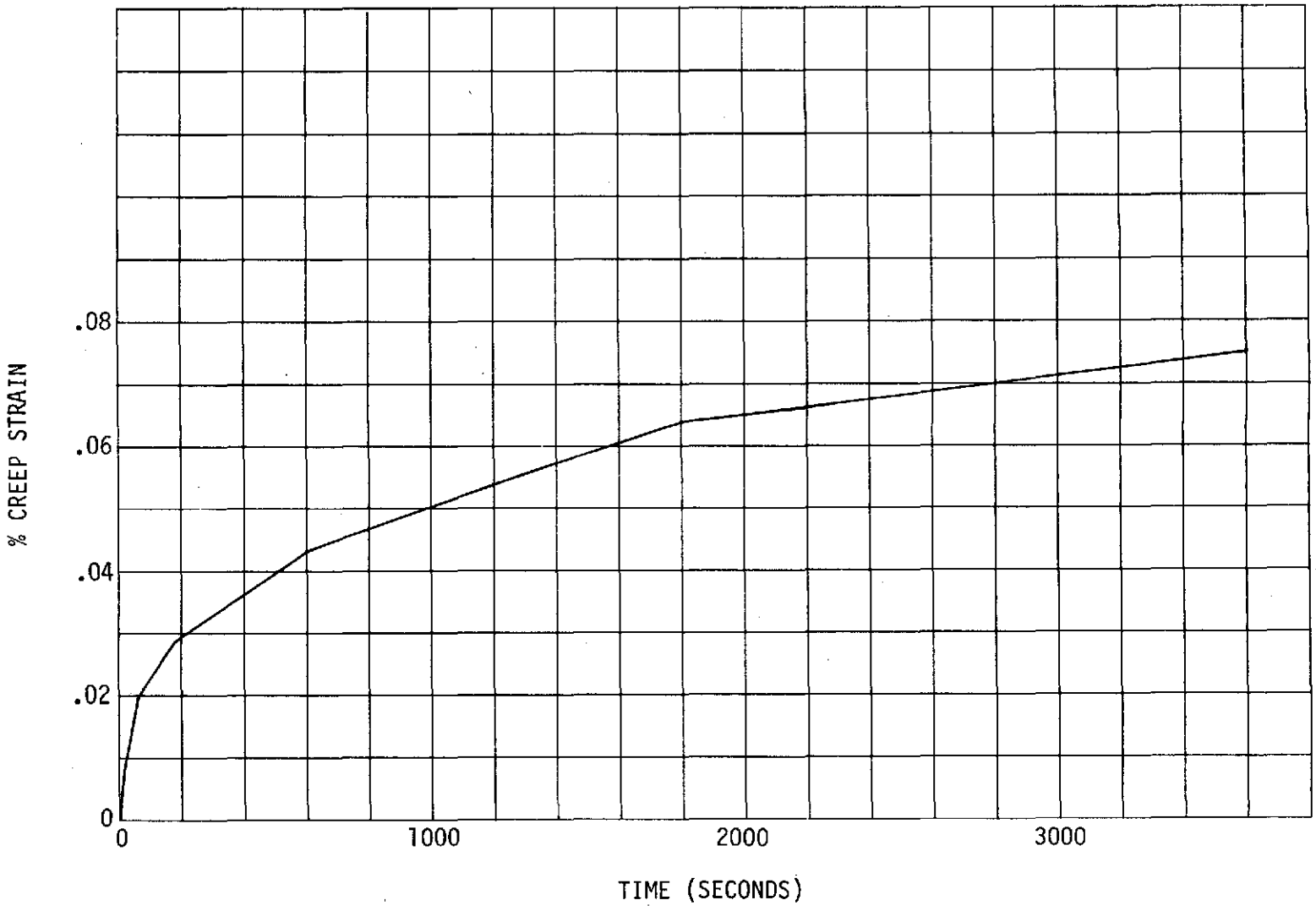

FIGURE 1.5-4: REFERENCE CREEP STRAIN VERSUS TIME

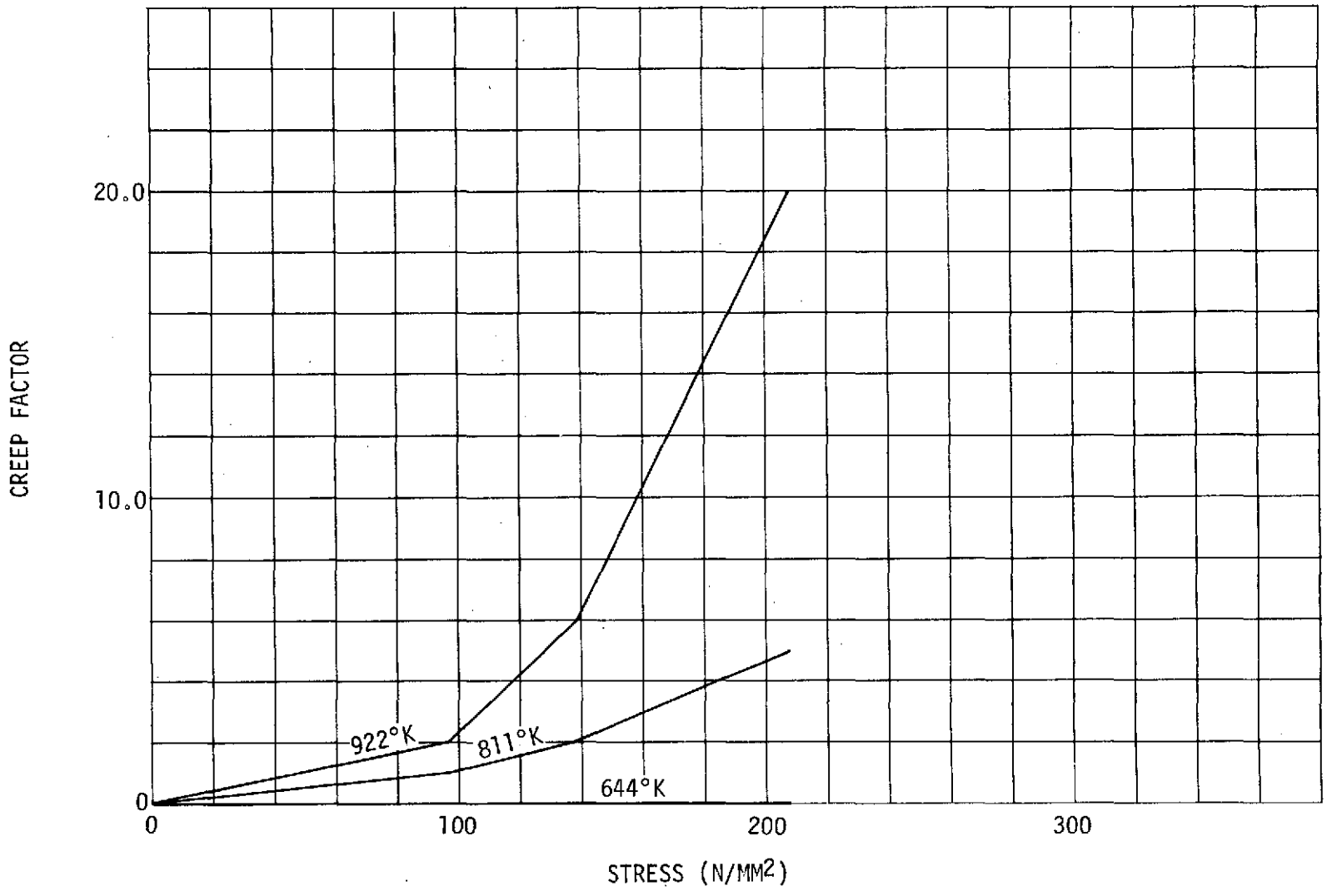

FIGURE 1.5-5: CREEP FACTOR VERSUS STRESS AND TEMPERATURE

THIS PAGE LEFT BLANK INTENTIONALLY.

2.0 THERMAL ANALYSIS

In order to provide temperature distributions as a function of time, it was necessary to perform a thermal analysis of the thrust chamber segment. The BETA II (Boeing Engineering Thermal Analyzer) thermal analyzer was used for this purpose. Previous thermal analysis of the SSME (Reference 10) configuration indicates that the start transient is characterized by two important conditions. A time t = 1.75 sec (see Figure 1.3-1), a "quasi-steady" condition, exists which corresponds to the low point in the coolant temperature start transient. The other important condition is the steady state operating condition reached at time t = 5.0 sec. For purposes of demonstration, temperatures are assumed to vary linearly from the initial condition to the cold point at t = 1.75 sec. and again linearly up to the operating condition at t = 5.0 sec. The steady condition is held for 500 sec. and the structural temperatures are then assumed to decrease linearly to a uniform 89°K (-300°F) during shutdown. The cycle is completed by a linear variation of temperatures back to the initial condition.

The lumped mass thermal model used for the thermal analysis is shown on Figure 2.0-1 with the numbered points indicating the locations where temperatures were determined. The appropriate boundary conditions are also shown on Figure 2.0-1. Along the radial lines of symmetry, and along the outside wall of the Inconel 718 jacket, a condition of zero heat transfer was assumed. On the hot gas wall, the temperature was specified. A specified coolant temperature along with a film coefficient computed at

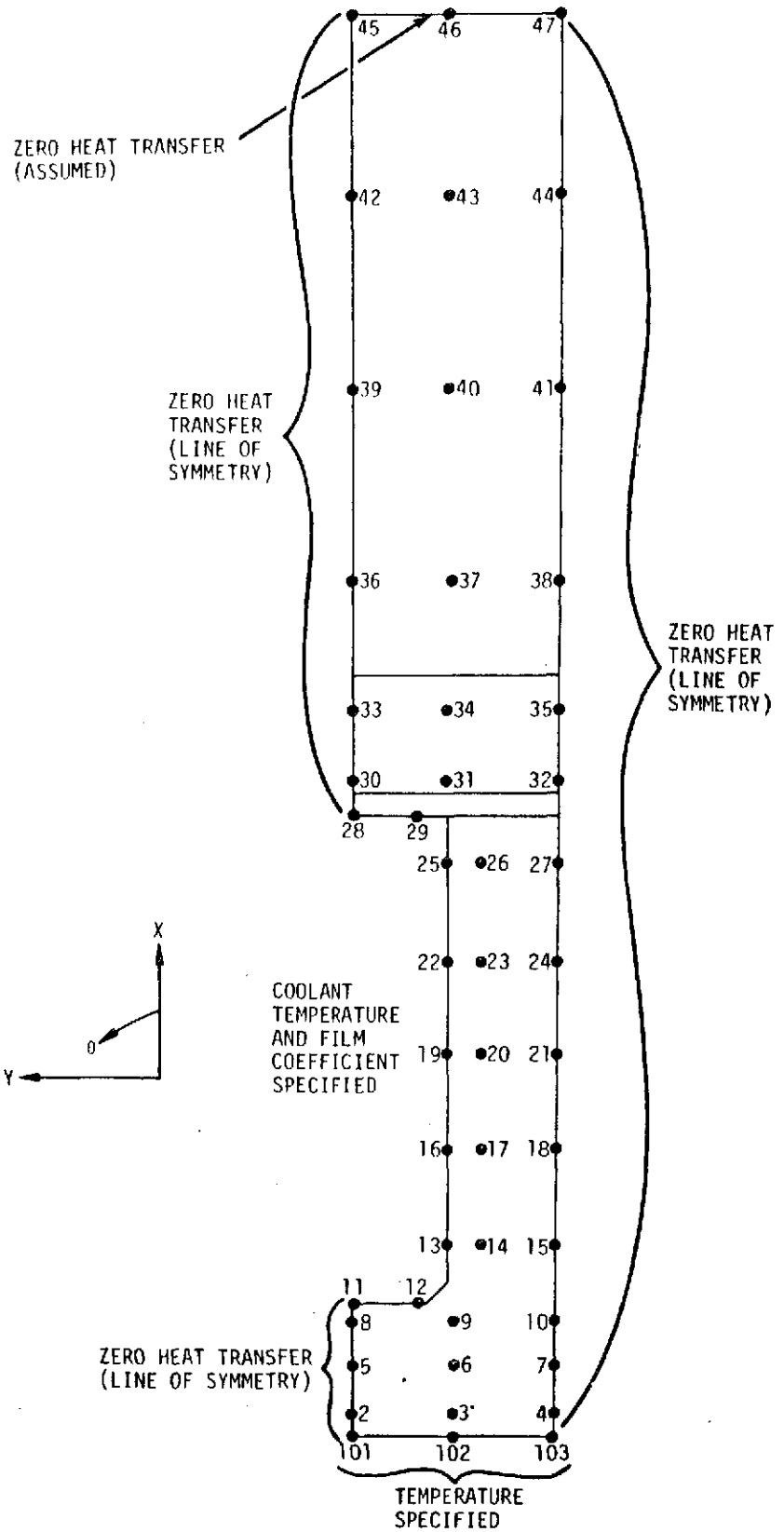

FIGURE 2.0-1: THERMAL MODEL

2.0 (Continued)

points around the coolant channel complete the required boundary conditions. The expression for the coolant film coefficient is (Reference 8)

$$h_c = (1.124 \times 10^{-5}) \frac{\lambda_c}{D_c} Re_c^{.8} Pr_c^{.4} \left(\frac{T_c}{Tw_c}\right)^{.55} \eta_E \left[\frac{BTU}{FT^2\text{-}SEC°R}\right]$$

where $D_c = 2\left(\frac{\text{Channel Area}}{\pi}\right)^{1/2}$

λ_c = Coolant thermal conductivity

Re_c = Coolant Reynolds number based on D_c

Pr_c = Coolant Prandtl number based on Tc, Pc

T_c = Coolant temperature (°R)

Tw_c = Local wall temperature at points around coolant channel (°R)

η_E = Enhancement factor due to surface roughness (Assumed $\eta_E = 1$)

Pc = Coolant passage static pressure

With values of coolant temperature and pressure given as functions of time during the start transient, it is convenient to define a function f(t) such that the film coefficient is a function of local wall temperature and time,

$$h_c(Tw_c, t) = \frac{f(t)}{Tw_c^{.55}}$$

2.0 (Continued)

where

$$f(t) = 1.124 \times 10^{-5} \frac{\lambda_c}{D_c} Re_c^{.8} Pr_c^{.4} T_c^{.55} \quad \left[\frac{BTU}{FT^2\text{-}SEC°R} (°F)^{.55} \right]$$

Figure 2.0-2 shows the variation of f(t) for the start transient defined by Figures 1.2-1, 1.3-1 and 1.4-1.

The results of the two steady state anslyses are shown in Figures 2.0-3 and 2.0-4. Figure 2.0-3 shows the thermal temperatures for t = 1.75 seconds and Figure 2.0-4 shows the thermal node temperatures for t = 5.0 seconds. The results of the thermal analysis were used as input data for the program INPUTB (Reference 11). The INPUTB program was used to generate finite element temperatures at selected times for input to BOPACE.

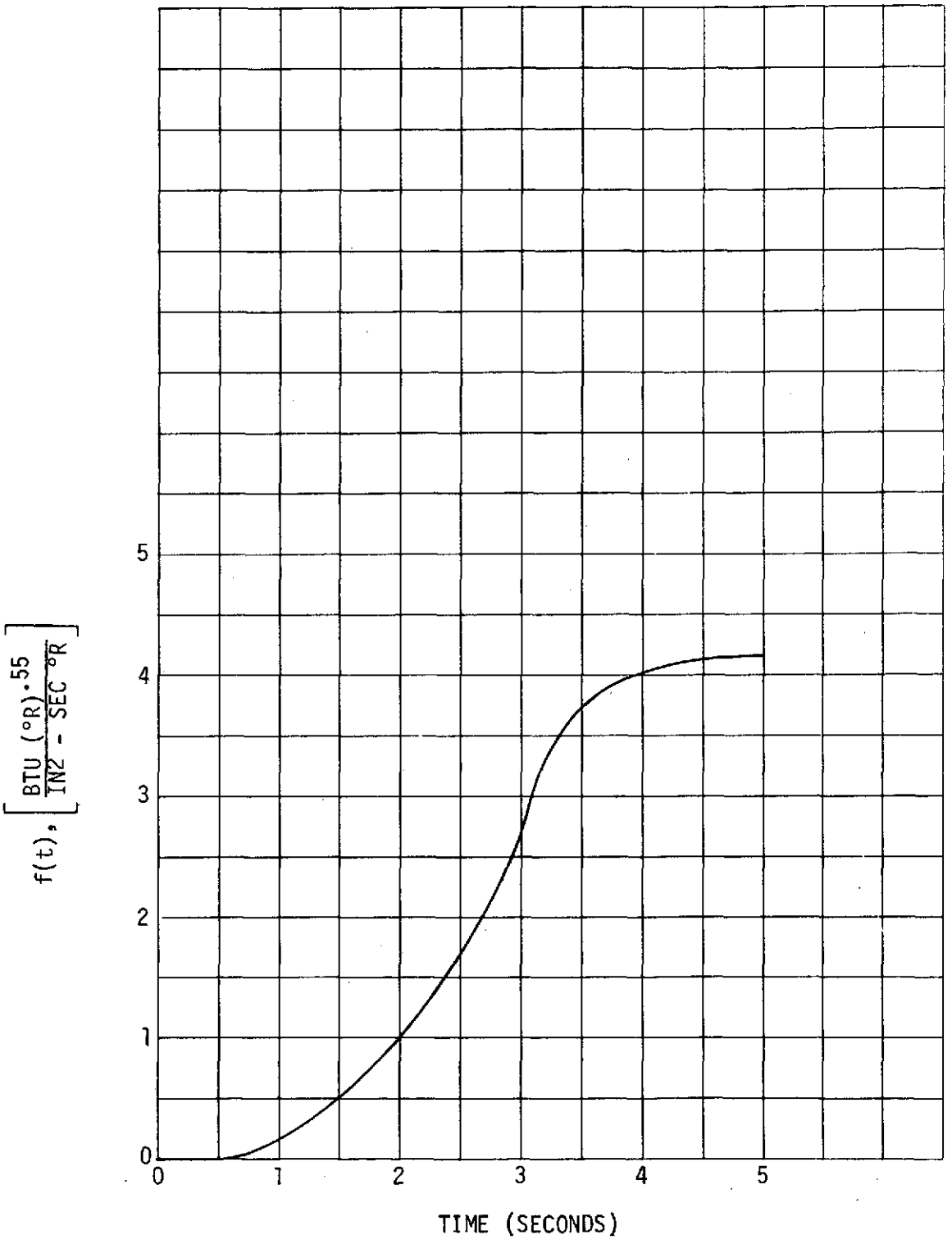

FIGURE 2.0-2: FILM COEFFICIENT FUNCTION VERSUS TIME

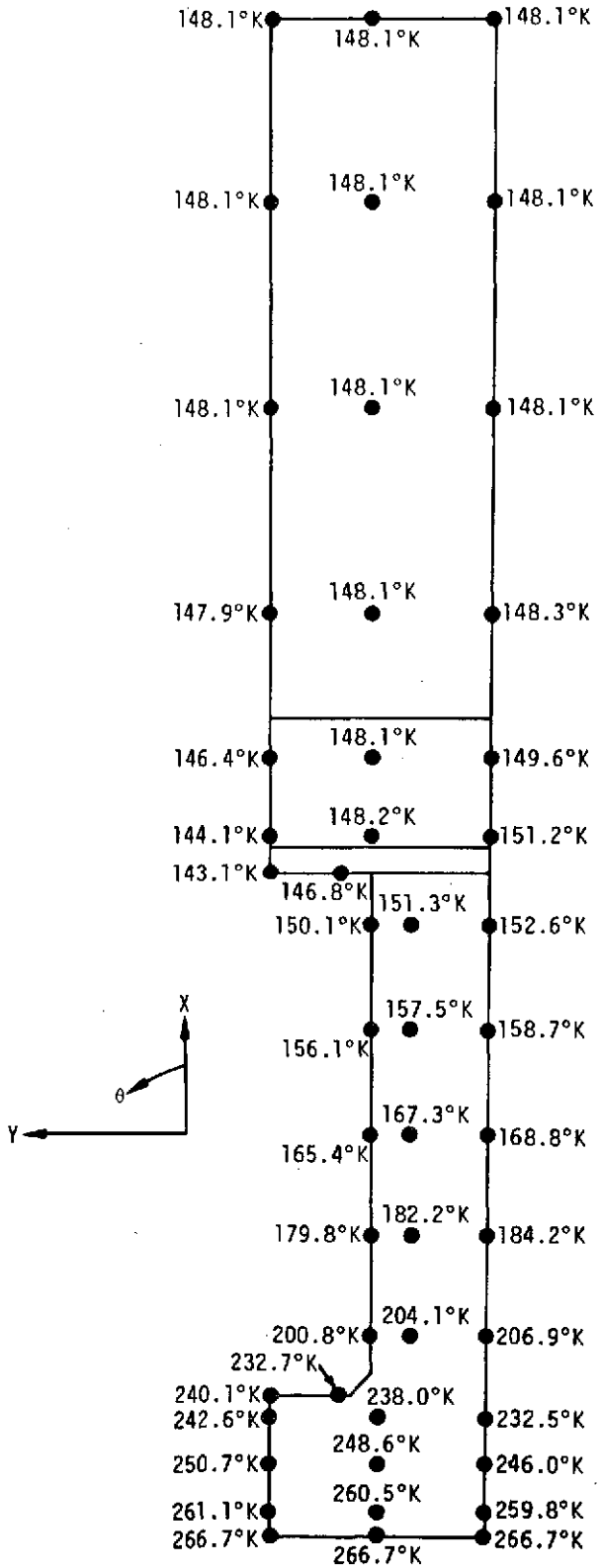

FIGURE 2.0-3: THERMAL NODE TEMPERATURES AT t = 1.75 SECONDS

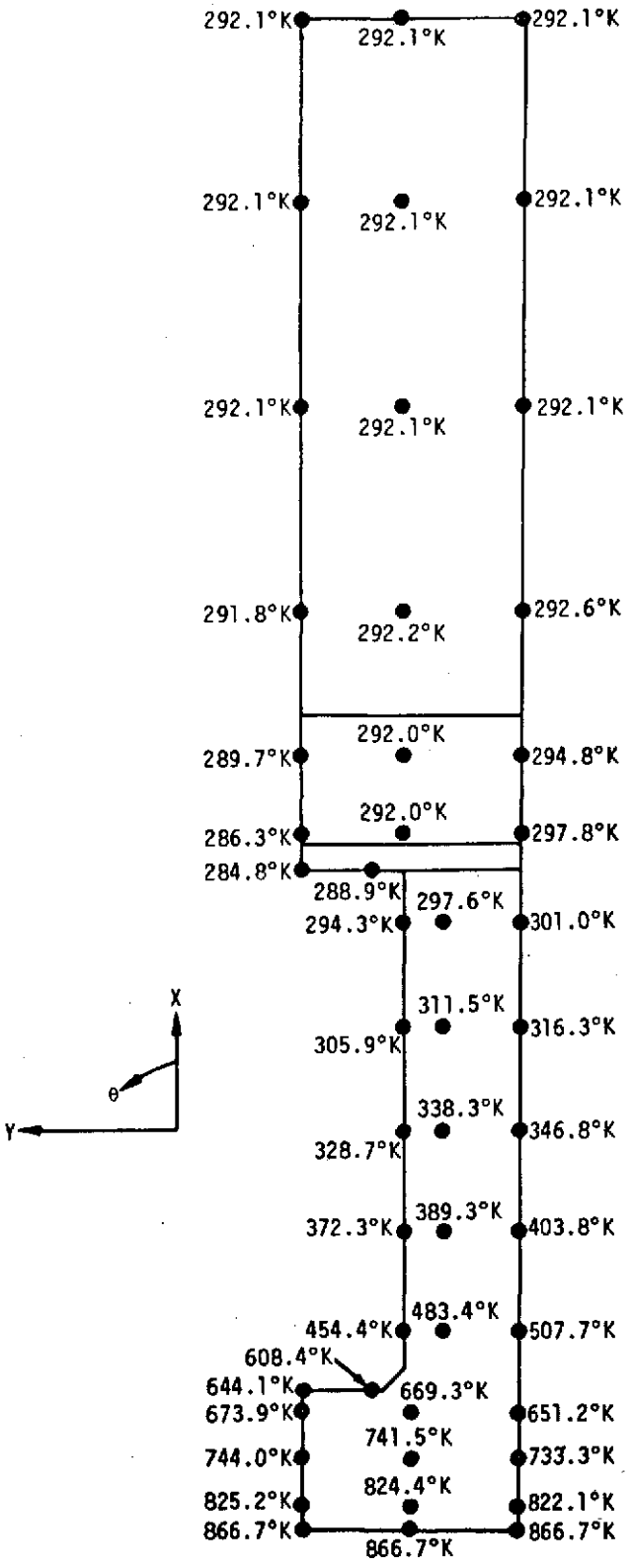

FIGURE 2.0-4: THERMAL NODE TEMPERATURES AT t = 5.0 SECONDS

THIS PAGE LEFT BLANK INTENTIONALLY.

3.0 FINITE ELEMENT MODEL

A 126 node, 184 element, constant-strain-triangle finite element model was developed to describe the thrust chamber segment shown on Figure 3.0-1. Figure 3.0-1 shows the model with the numbers identifying the elements. The size of the model was kept to a minimum without sacrificing detail in the area near the hot gas wall.

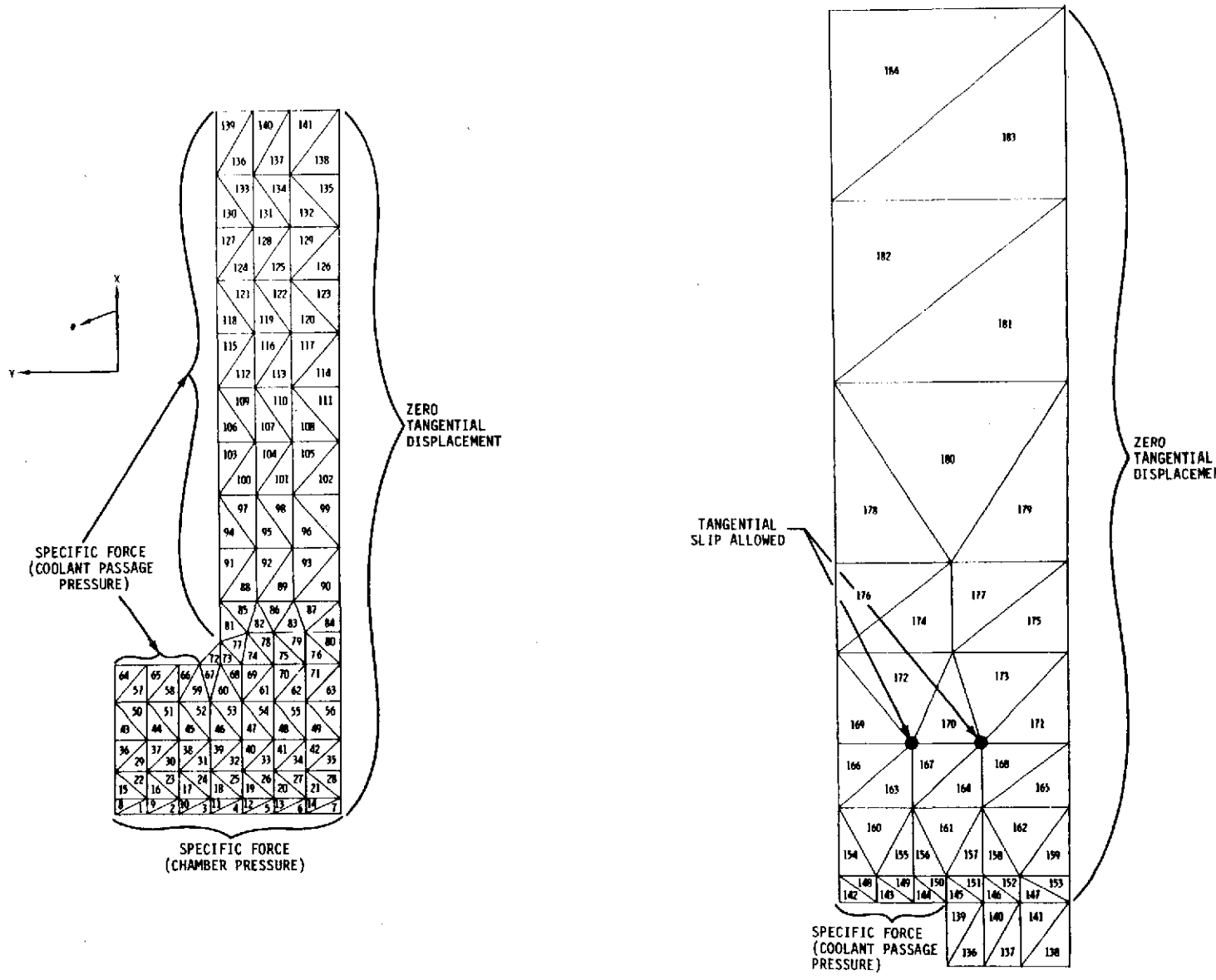

FIGURE 3.0-1: FINITE ELEMENT MODEL

4.0 RESULTS

The results of the analysis are conveniently summarized in terms of contour plots of important quantities at significant times during the engine cycle. In addition, plots of important quantities as a function of time illustrate the cyclic variations that the structure experiences.

4.1 CONTOUR PLOTS AT SELECTED TIMES

Table 4.1-1 lists the contour plots which were prepared along with a description of their significance.

TABLE 4.1-1

SUMMARY OF CONTOUR PLOTS

FIGURE	QUANTITY PLOTTED	CYCLE/ TIME(SEC)	DESCRIPTION
4.1-1	T	1/1.75	Initial cooling of structure causes plastic deformation of EFCU.
4.1-2	ε^{P}_{EFF}	1/1.75	
4.1-3	T	1/5.0	EPL operating temperatures (hold from t = 5.0 to 505.)
4.1-4	σ_{EFF}	1/5.0	Stress levels prior to sustained burn.
4.1-5	ε^{P}_{EFF}	1/505.	Plastic strains at end of 500 sec. burn; largest strains are radial (XX).
4.1-6	ε^{P}_{XX}	1/505.	
4.1-7	ε^{P}_{YY}	1/505.	
4.1-8	ε^{C}_{EFF}	1/505.	Creep strains at end of 500 sec. hold.
4.1-9	σ_{EFF}	1/505.	Effective stresses at end of 500 sec. hold showing relaxation due to creep.
4.1-10	ε^{P}_{EFF}	1/506.4	Plastic strains at end of shutdown (T = 89°K Uniform).
4.1-11	ε^{P}_{EFF}	1/510.	Residual plastic strains at end of first cycle.
4.1-12	ε^{C}_{EFF}	1/510.	Residual creep strains at end of first cycle.
4.1-13	ε^{P}_{EFF}	2/505.	Plastic and creep strains at end of 500 sec. burn for second cycle; note change from first cycle.
4.1-14	ε^{C}_{EFF}	2/505.	
4.1-15	ε^{P}_{EFF}	2/510.	Residual plastic and creep strains at end of second cycle; note growth of residual strains.
4.1-16	ε^{C}_{EFF}	2/510.	

TABLE 4.1-1

SUMMARY OF CONTOUR PLOTS (CONTINUED)

FIGURE	QUANTITY PLOTTED	CYCLE/ TIME(SEC)	DESCRIPTION
4.1-17	ε^{P}_{EFF}	3/505.	Plastic and creep strains at end of 500 sec. burn for third cycle; note change from first cycle.
4.1-18	ε^{C}_{EFF}	3/505.	
4.1-19	ε^{P}_{EFF}	3/510.	Residual plastic and creep strains at end of third cycle; note further growth of residual strains.
4.1-20	ε^{C}_{EFF}	3/510.	

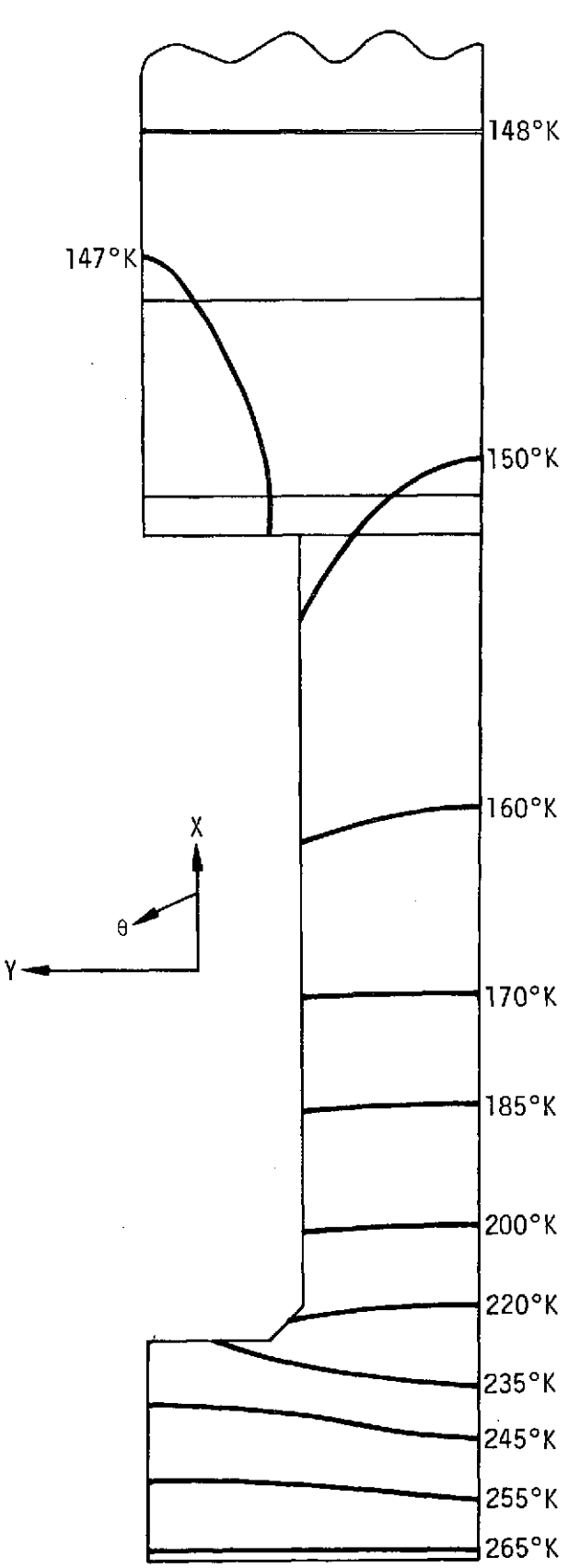

FIGURE 4.1-1: TEMPERATURE, CYCLE 1, t = 1.75 SEC.

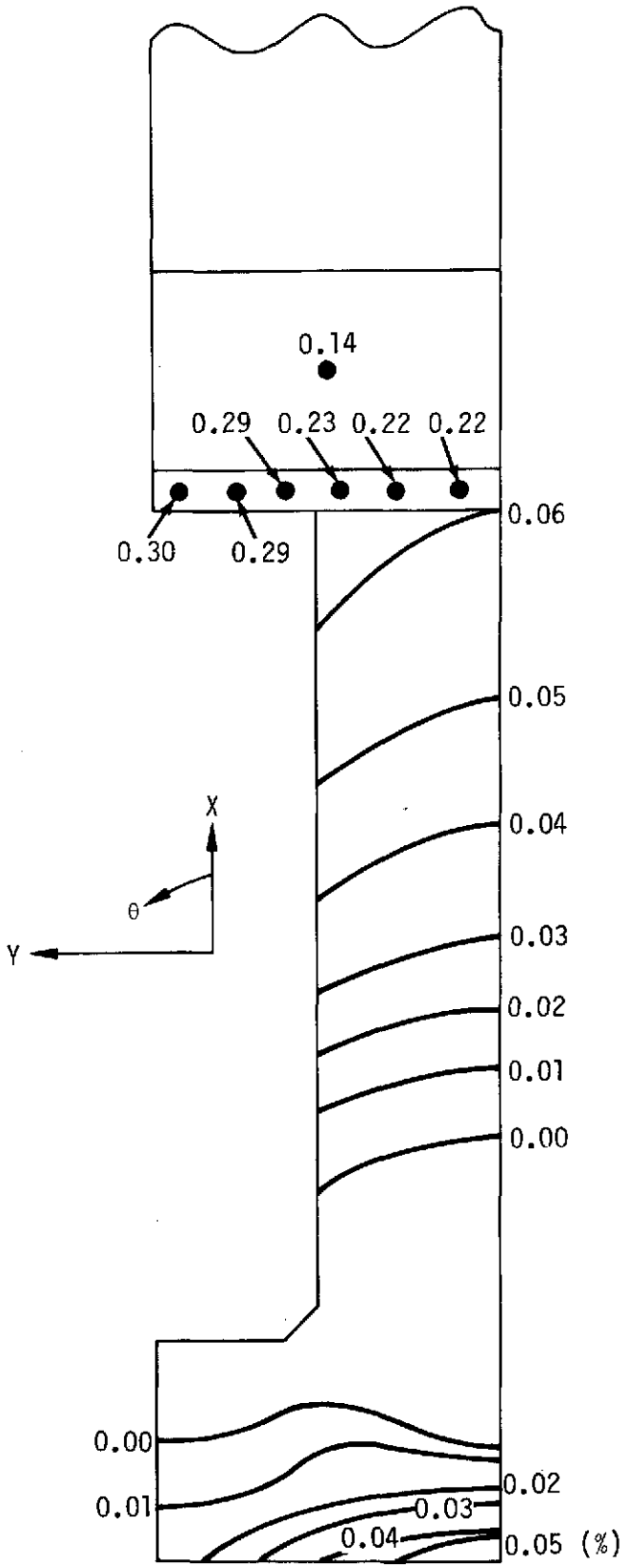

FIGURE 4.1-2: EFFECTIVE PLASTIC STRAIN, CYCLE 1, t = 1.75 SEC

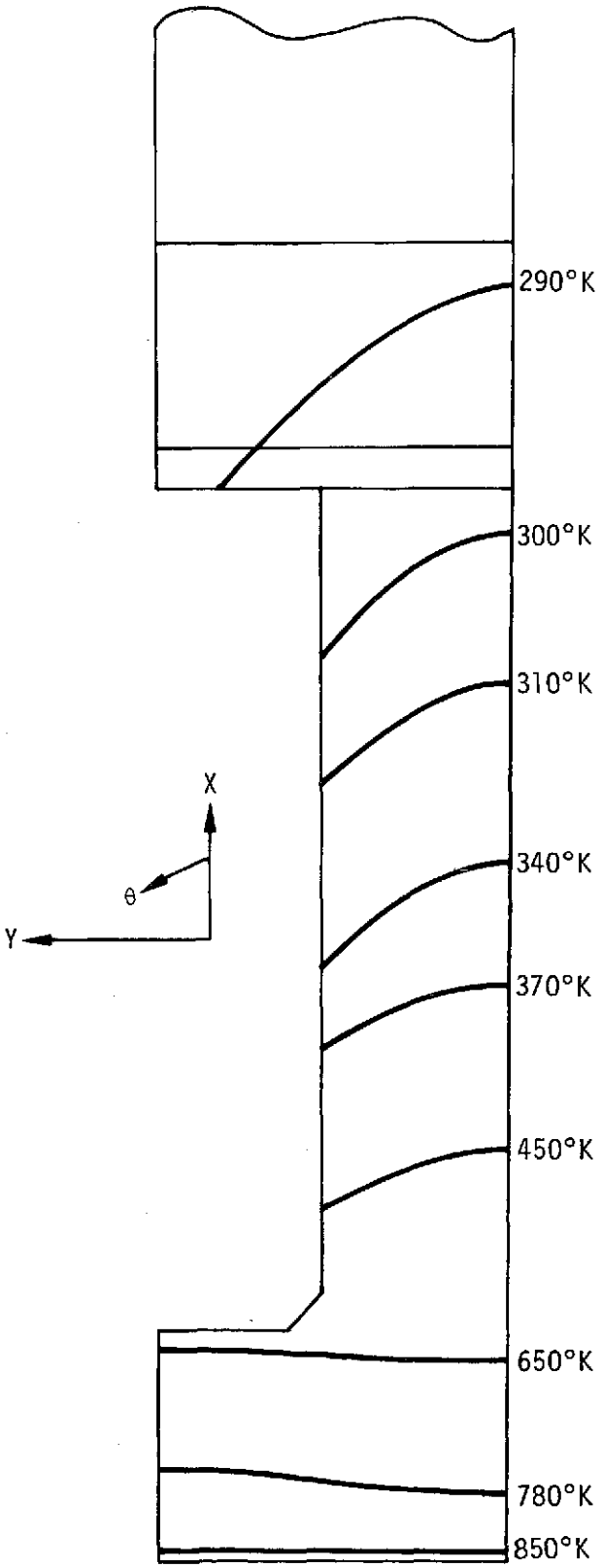

FIGURE 4.1-3: TEMPERATURE, CYCLE 1, t = 5.0 SEC.

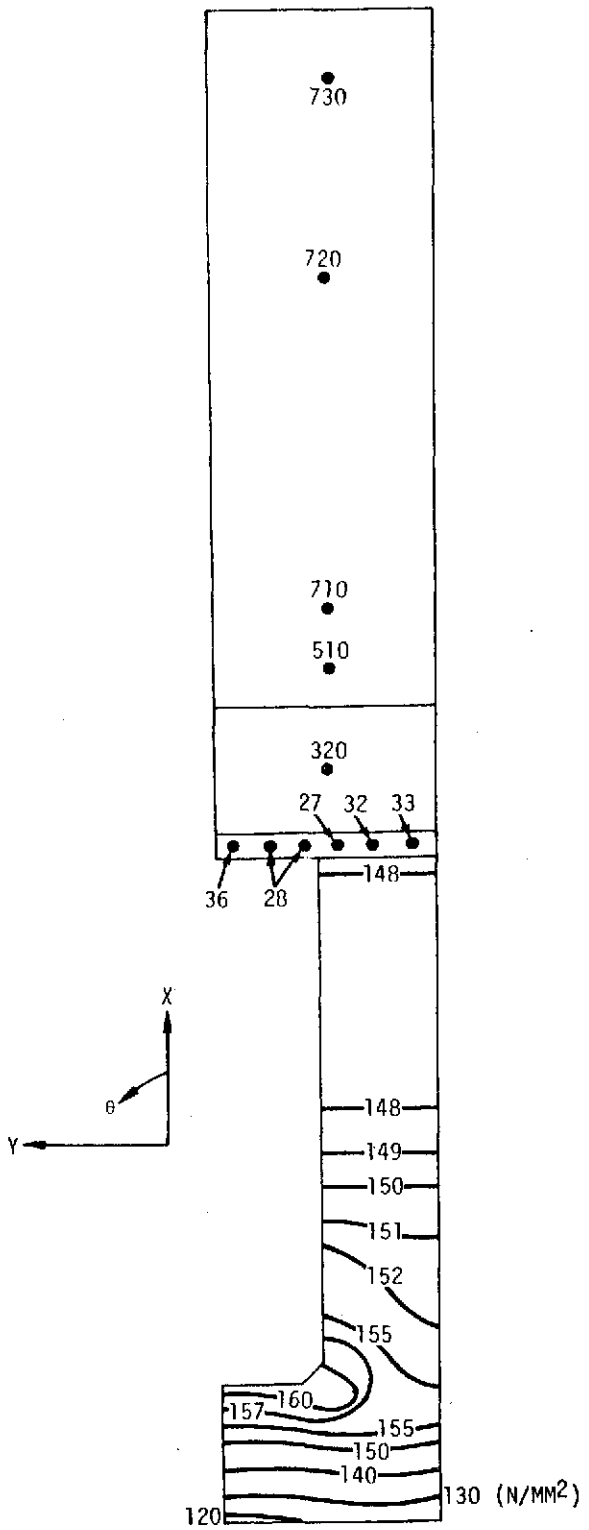

FIGURE 4.1-4: EFFECTIVE STRESS, CYCLE 1, t = 5.0 SEC.

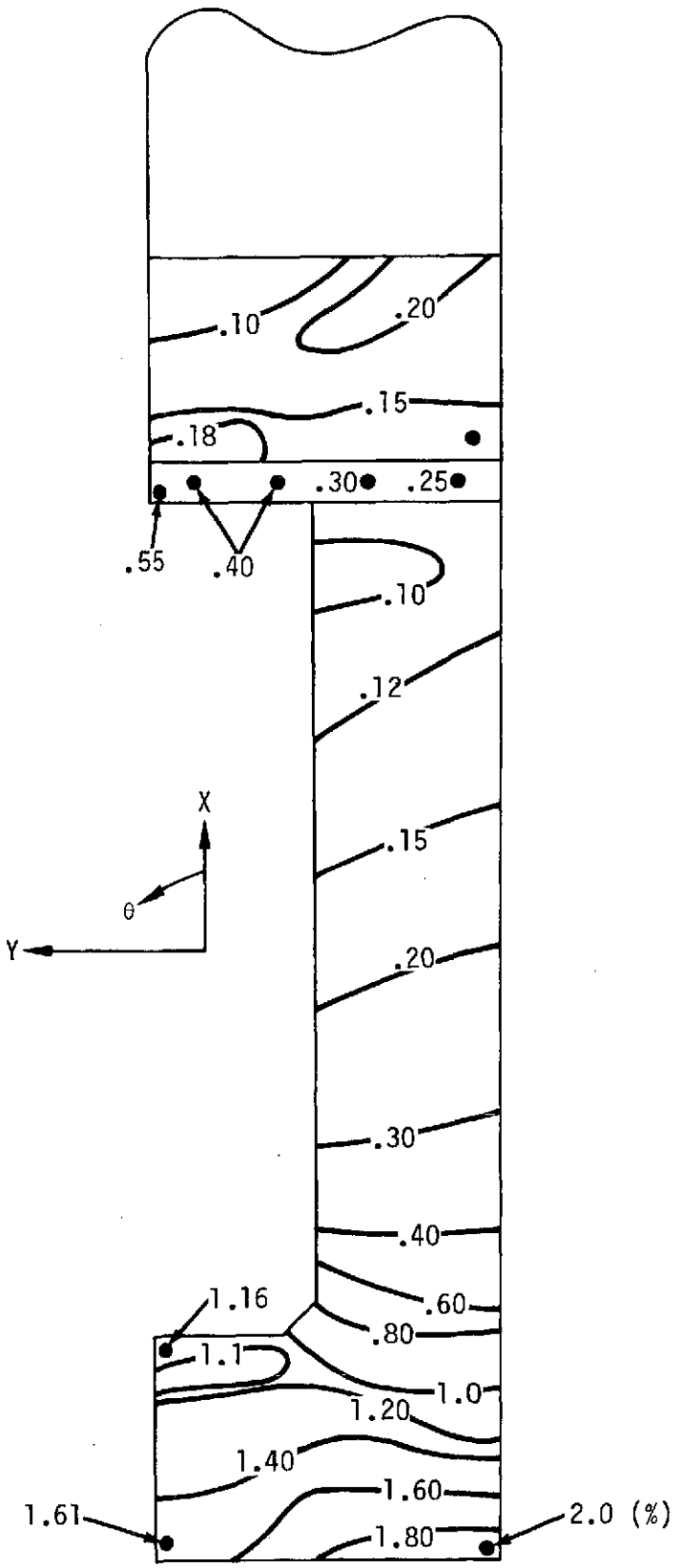

FIGURE 4.1-5: EFFECTIVE PLASTIC STRAIN, CYCLE 1, t = 1.75 SEC

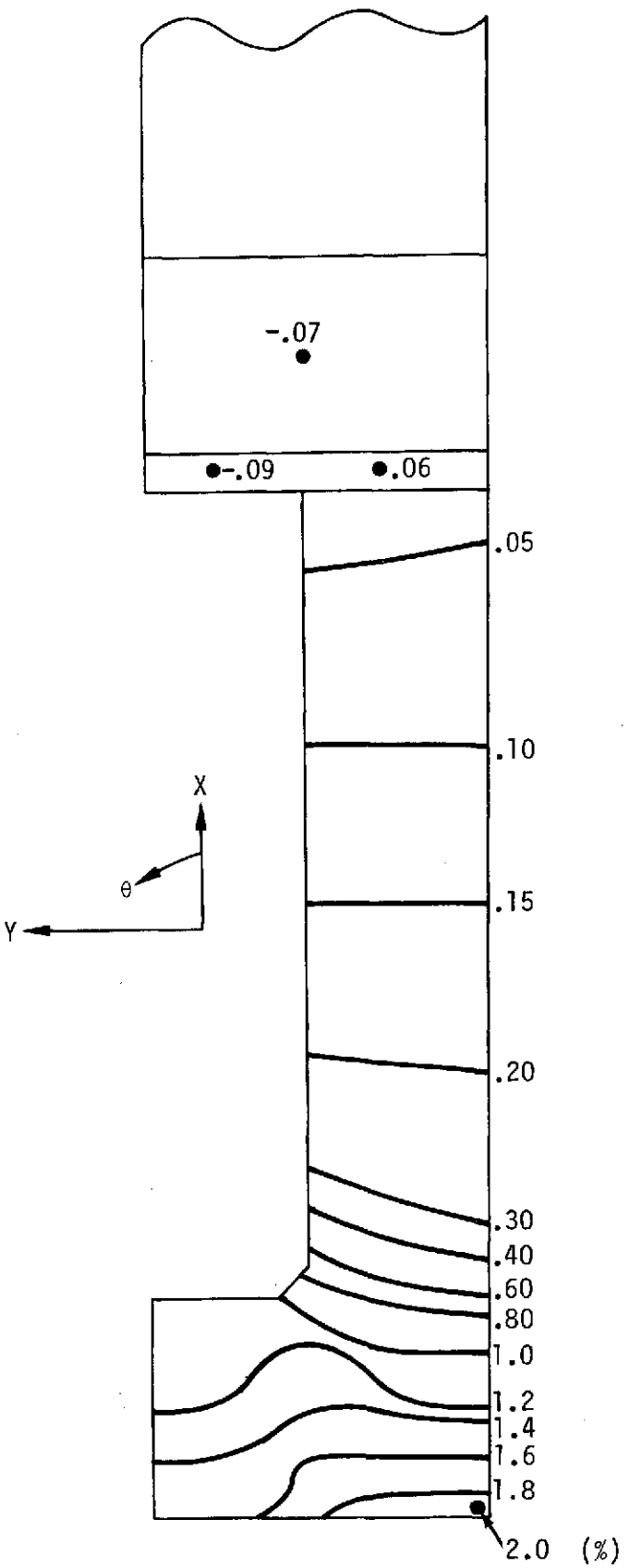

FIGURE 4.1-6: RADIAL PLASTIC STRAIN, CYCLE 1, t = 5.0 SEC

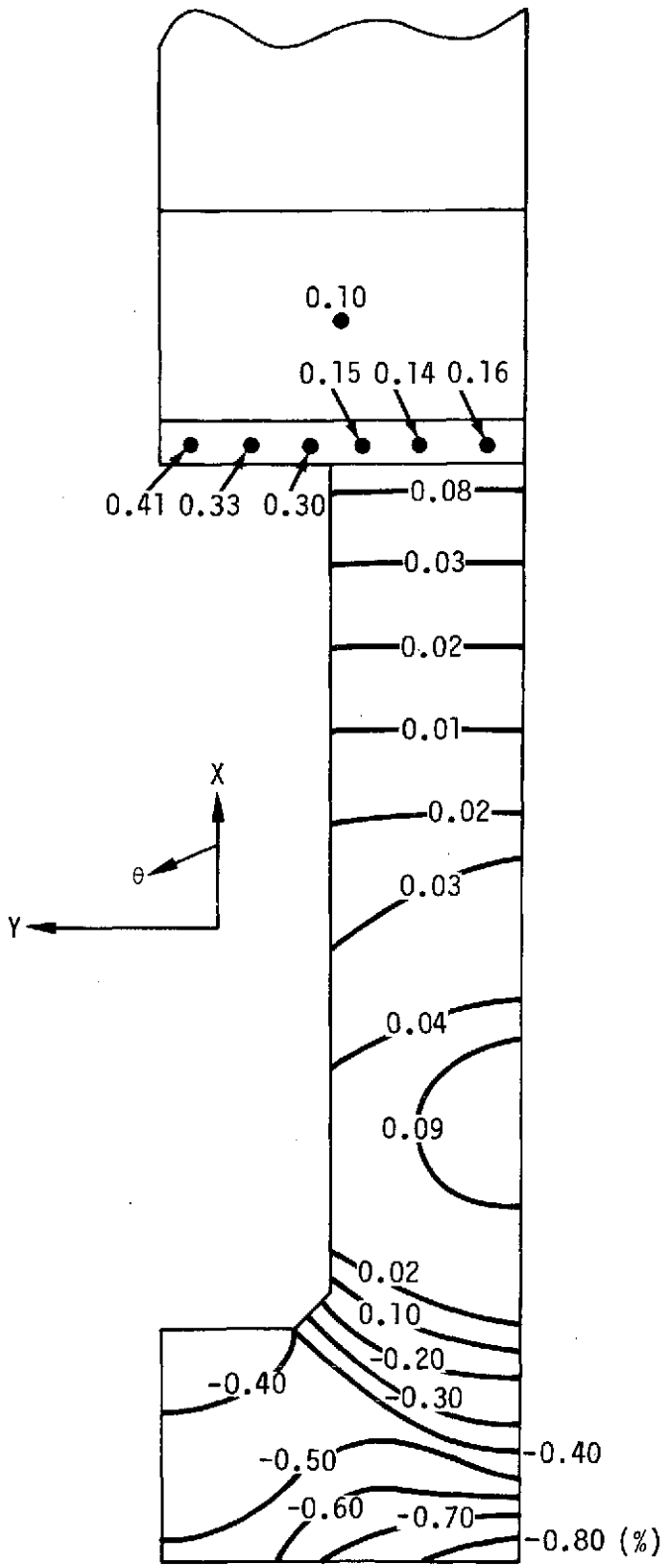

FIGURE 4.1-7: TANGENTIAL PLASTIC STRAIN, CYCLE 1, t = 505. SEC.

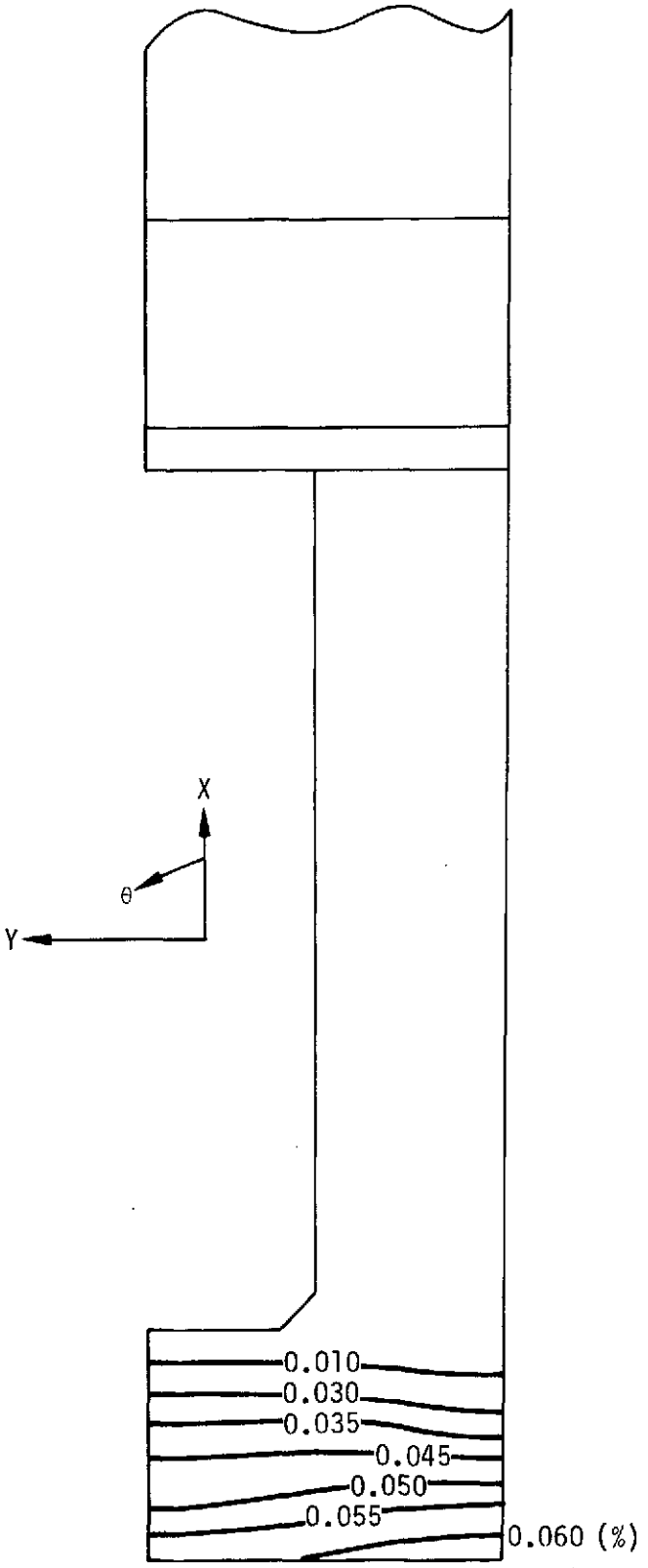

FIGURE 4.1-8: EFFECTIVE CREEP STRAIN, CYCLE 1, t = 505. SEC.

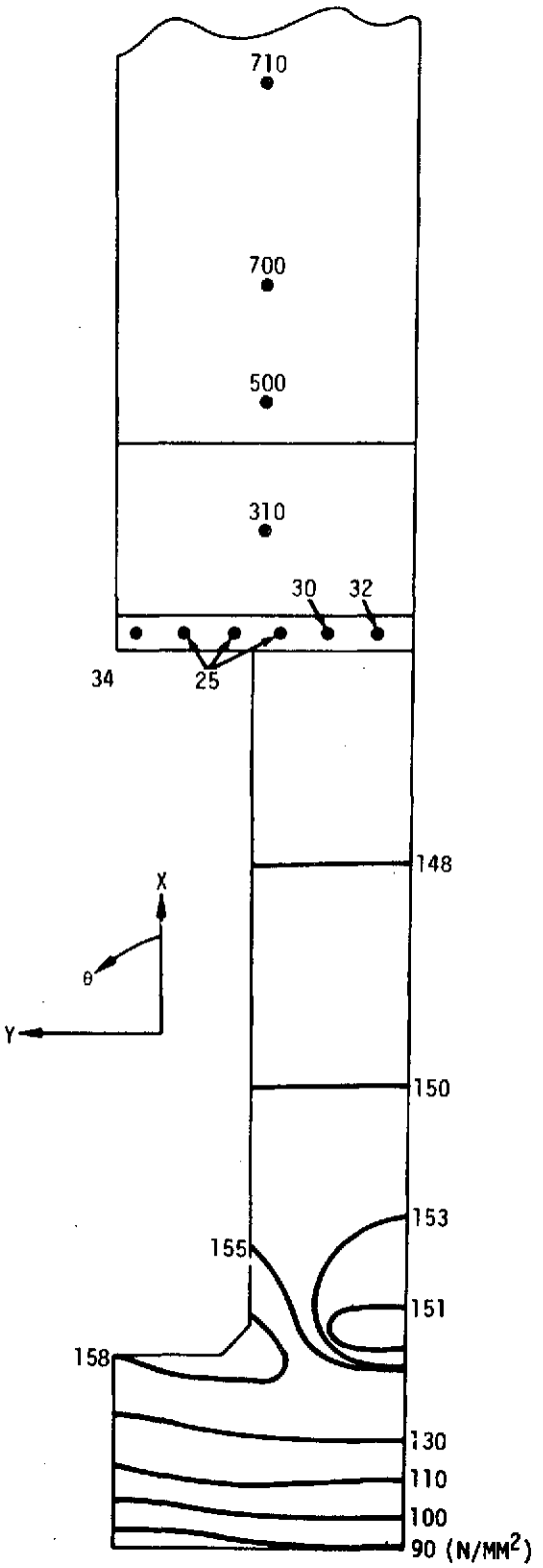

FIGURE 4.1-9: EFFECTIVE STRESS, CYCLE 1, t = 505. SEC.

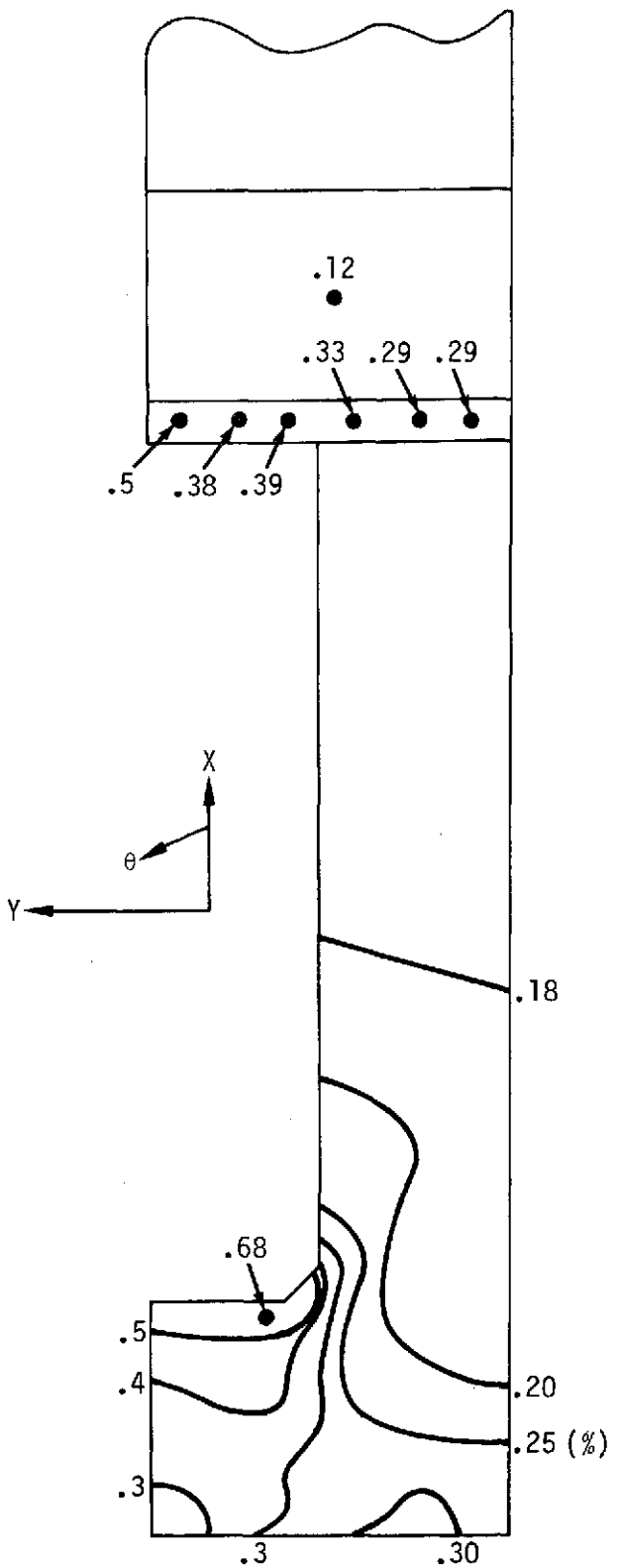

FIGURE 4.1-10: EFFECTIVE PLASTIC STRAIN, CYCLE 1, t = 506.4 SEC.

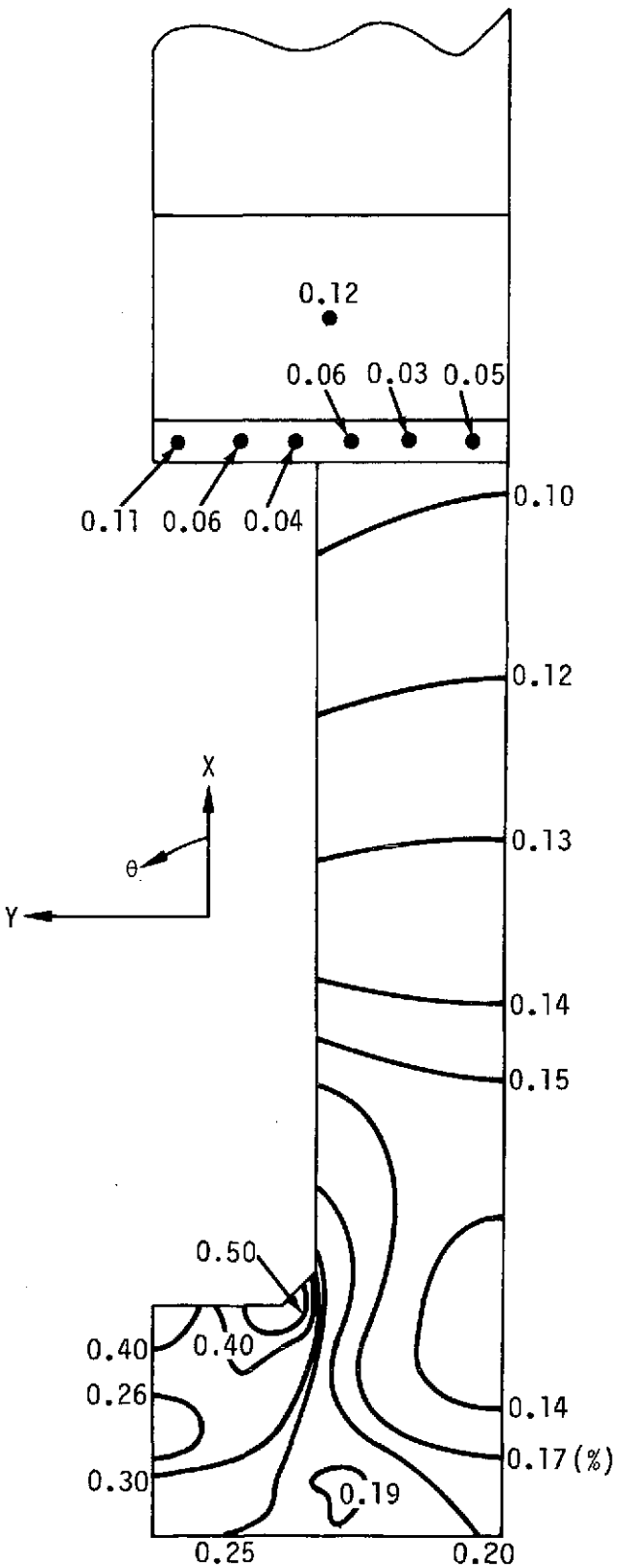

FIGURE 4.1-11: EFFECTIVE PLASTIC STRAIN, CYCLE 1, t = 510. SEC.

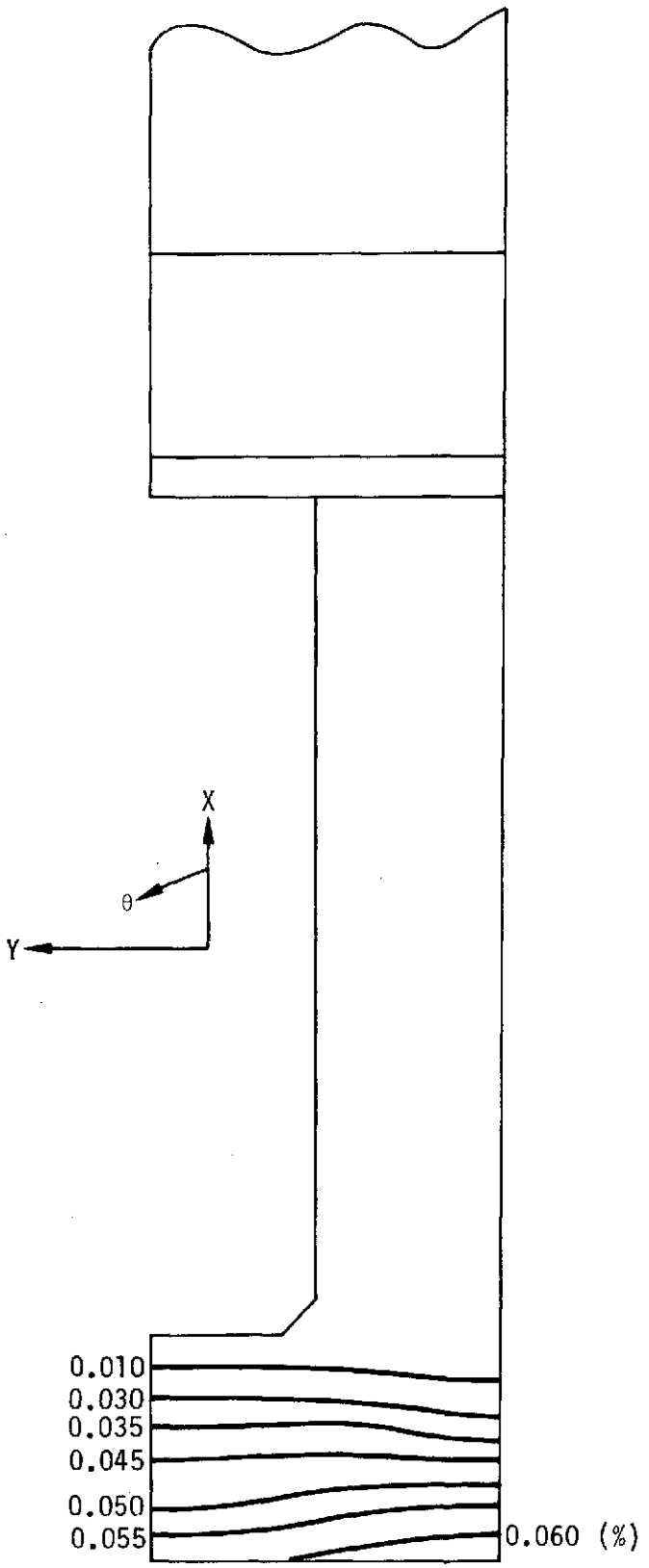

FIGURE 4.1-12: EFFECTIVE CREEP STRAIN, CYCLE 1, t = 510. SEC.

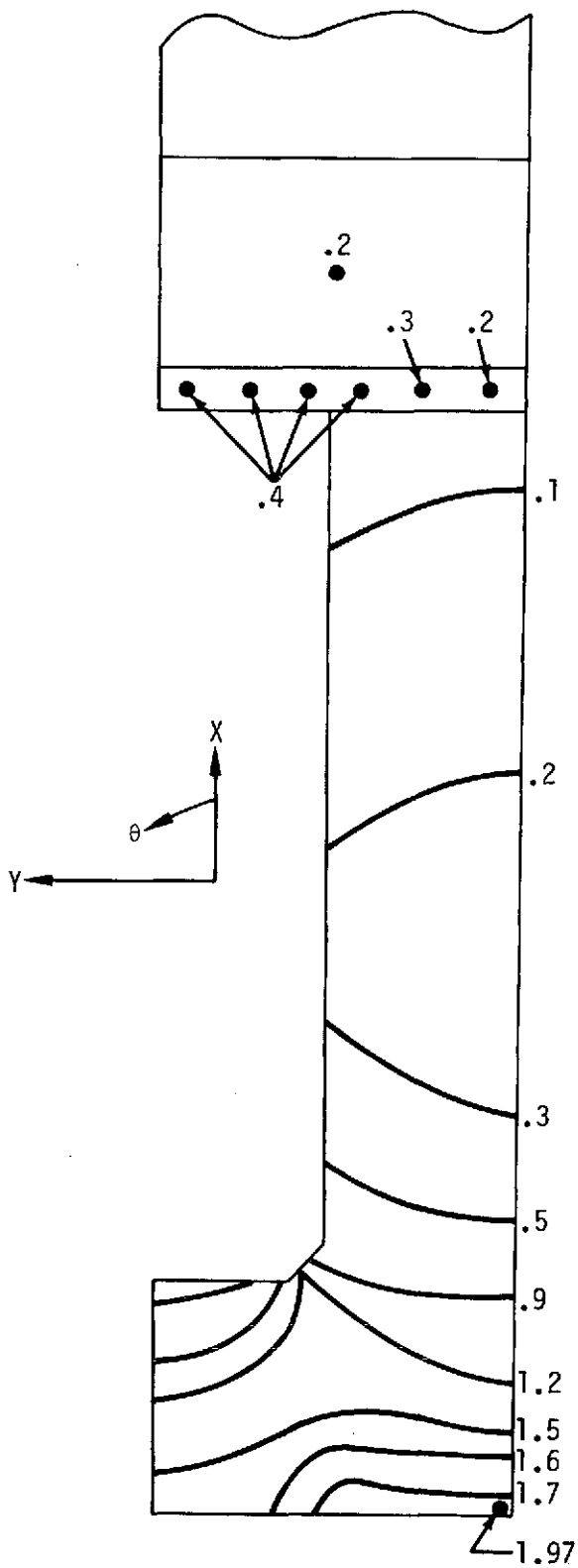

FIGURE 4.1-13: EFFECTIVE PLASTIC STRAIN, CYCLE 2, t = 505. SEC.

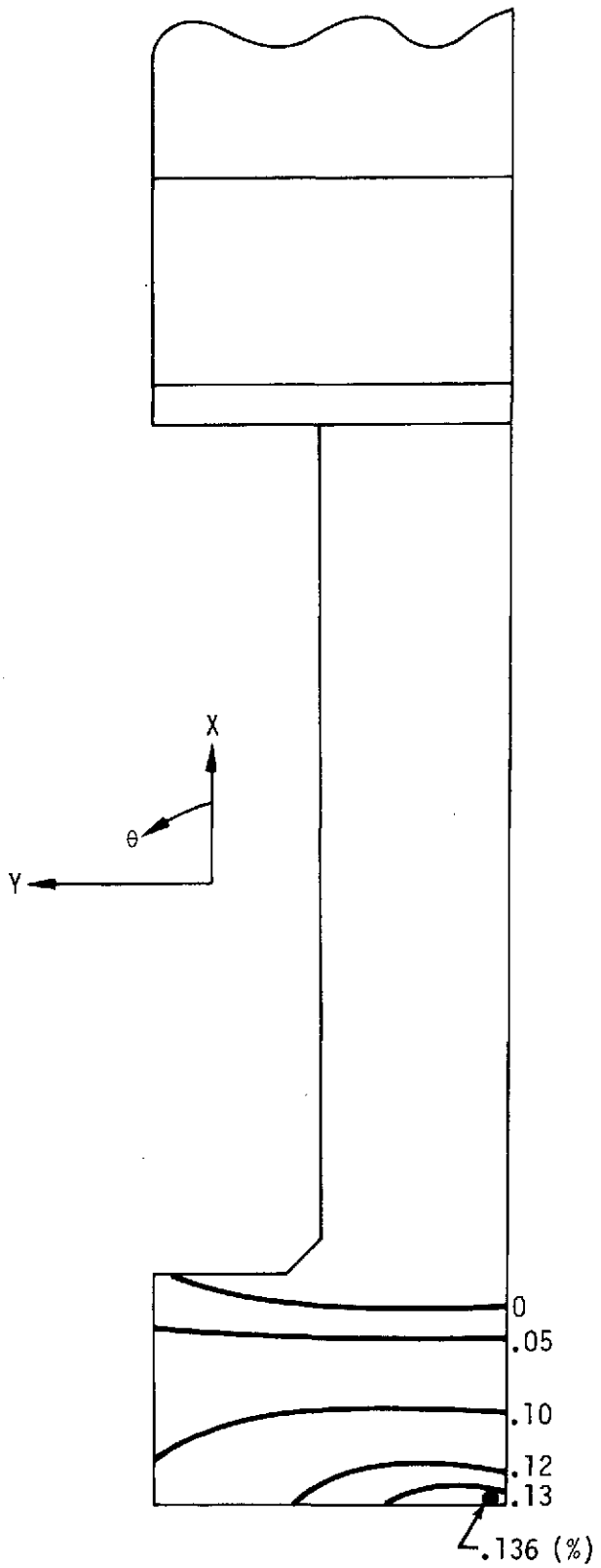

FIGURE 4.1-14: EFFECTIVE CREEP STRAIN, CYCLE 2, t = 505. SEC.

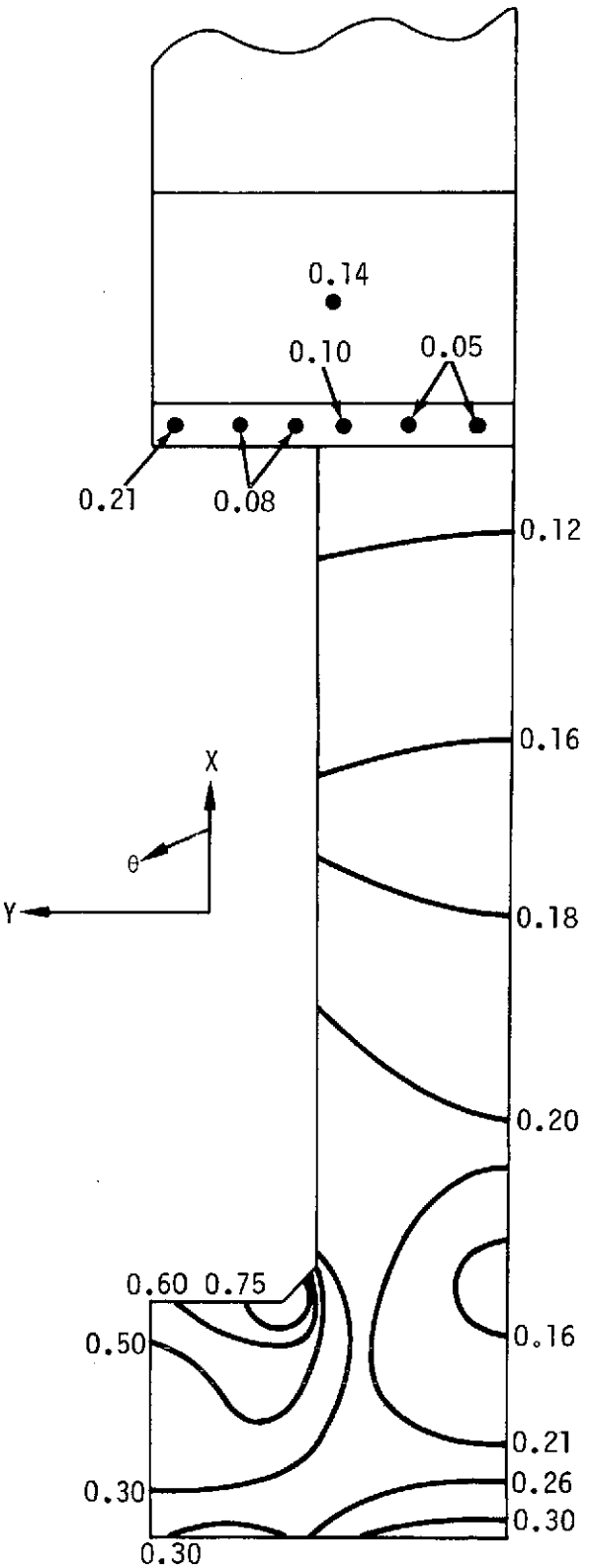

FIGURE 4.1-15: EFFECTIVE PLASTIC STRAIN, CYCLE 2, t = 510. SEC.

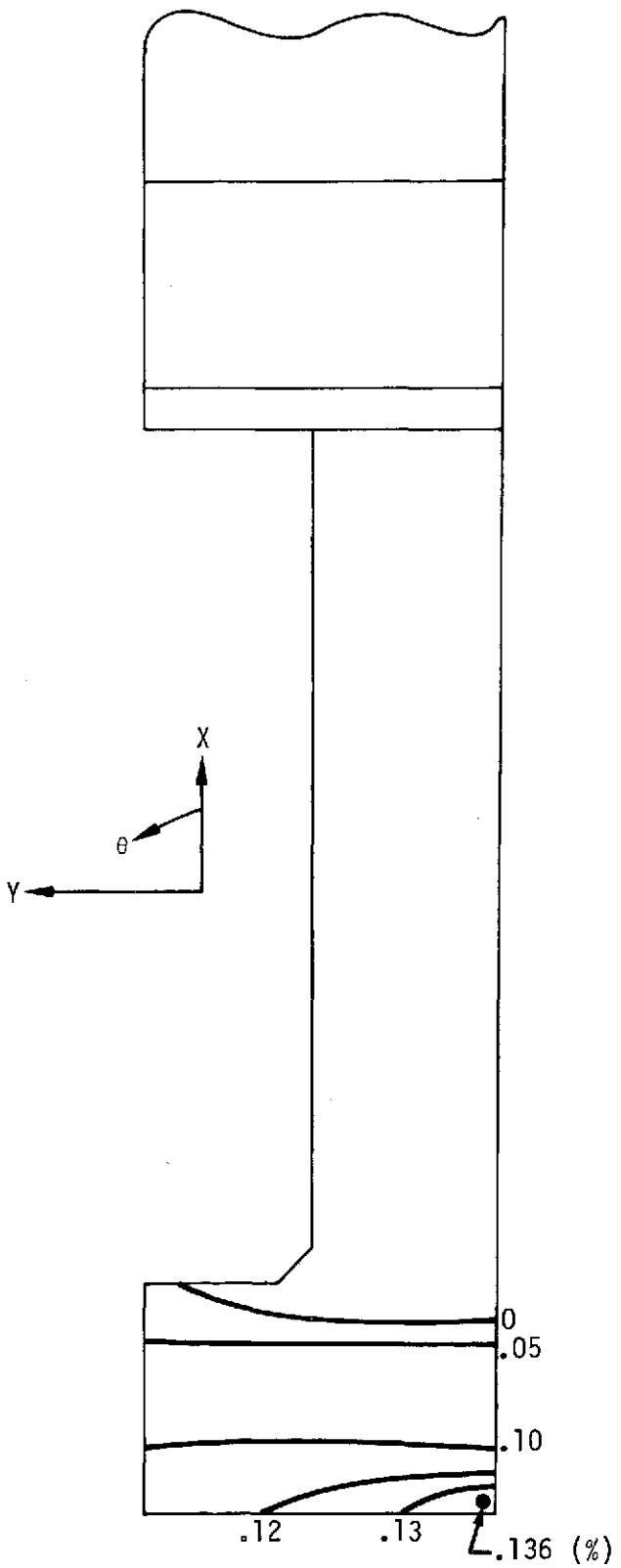

FIGURE 4.1-16: EFFECTIVE CREEP STRAIN, CYCLE 2, t = 510. SEC.

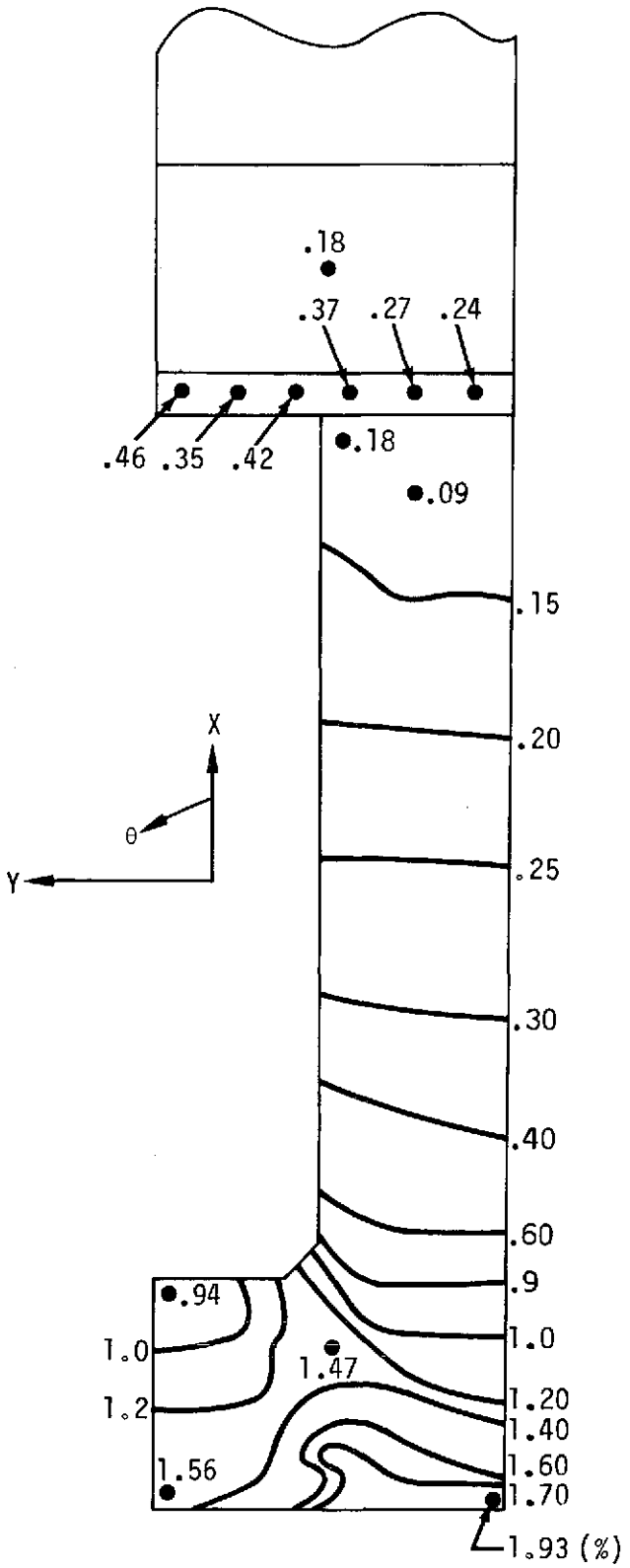

FIGURE 4.1-17: EFFECTIVE PLASTIC STRAIN, CYCLE 3, t = 505. SEC.

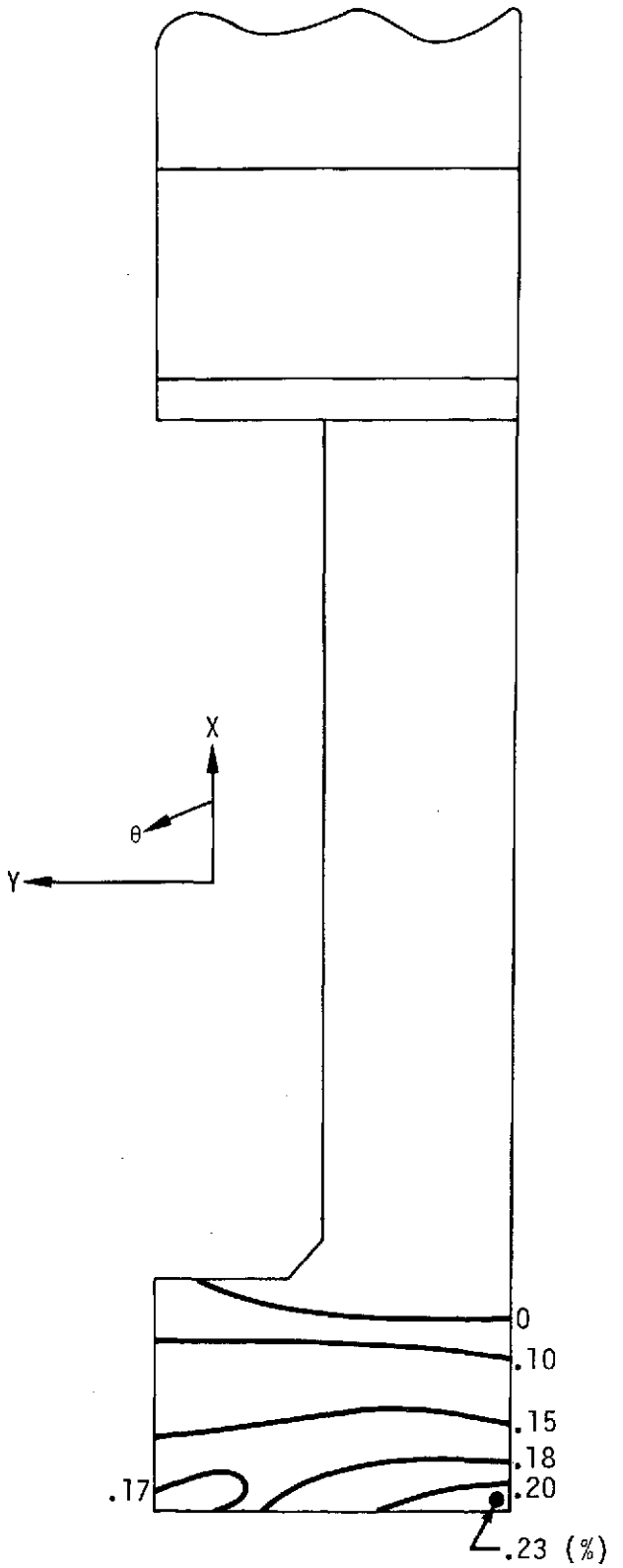

FIGURE 4.1-18: EFFECTIVE CREEP STRAIN, CYCLE 3, t = 505. SEC.

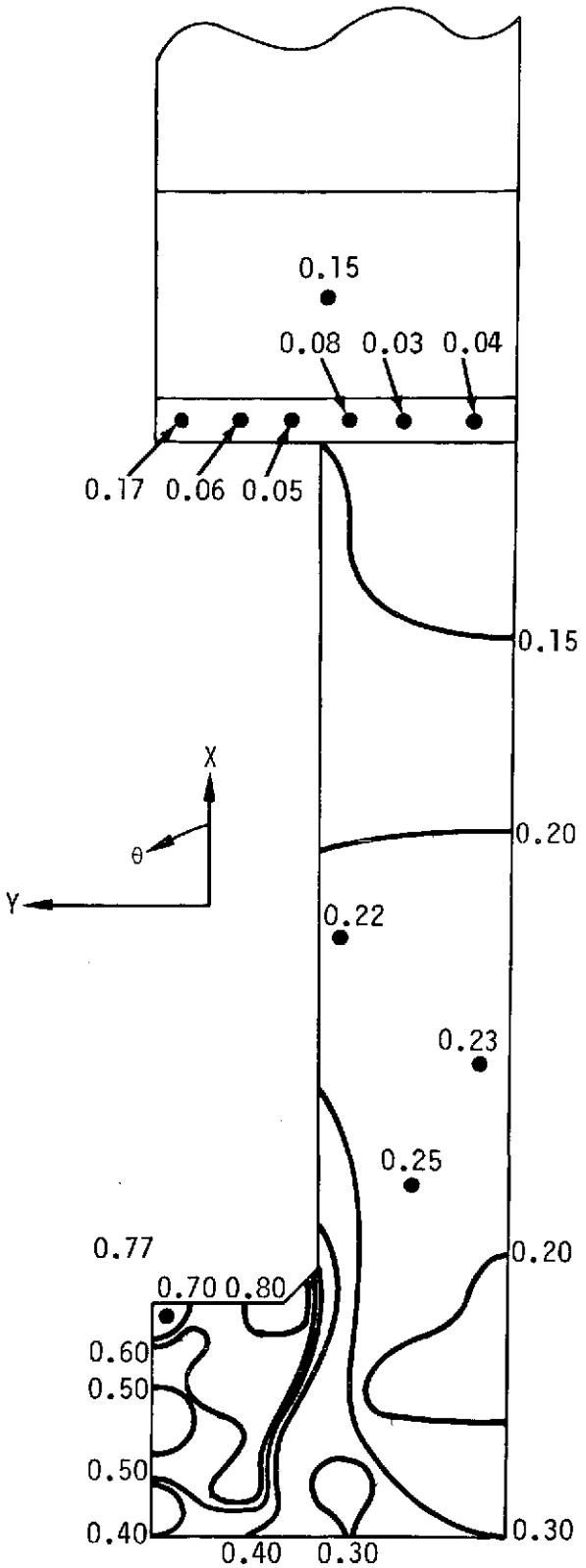

FIGURE 4.1-19: EFFECTIVE PLASTIC STRAIN, CYCLE 3, t = 510. SEC.

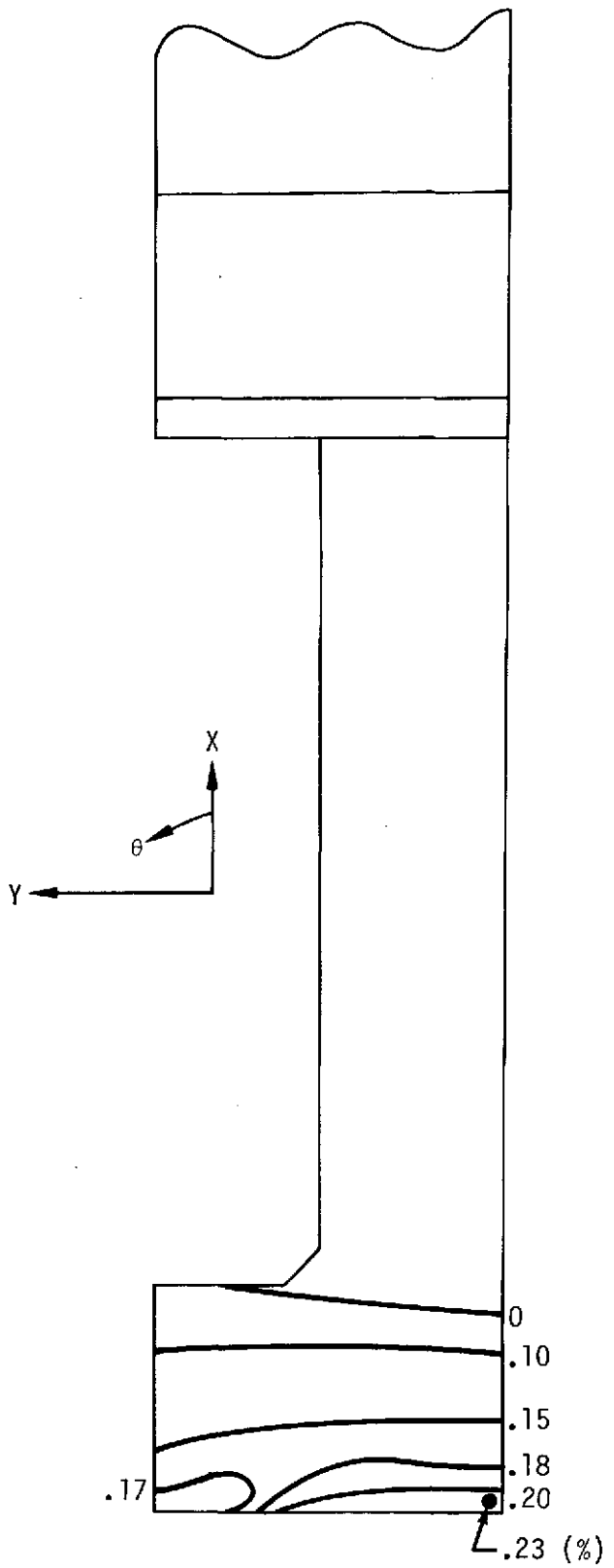

FIGURE 4.1-20: EFFECTIVE CREEP STRAIN, CYCLE 3, t = 510. SEC.

4.2 TIME HISTORIES OF SELECTED QUANTITIES FOR ELEMENT 7

Element 7 is the critical element for evaluation of the fatigue life of the thrust chamber liner since it undergoes the largest plastic deformation. The following quantities reflect the force-displacement-temperature history of element 7. They are listed along with the Figures on which they appear:

TEMP	FIGURE 4.2-1
ε^P_{XX}, ε^P_{YY}, ε^P_{ZZ}	FIGURE 4.2-2
ε^P_{EFF}, $\sum\Delta\varepsilon^P_{EFF}$	FIGURE 4.2-3
σ_{YY}, σ_{ZZ}, σ_{EFF}	FIGURE 4.2-4
ε^C_{EFF}	FIGURE 4.2-5

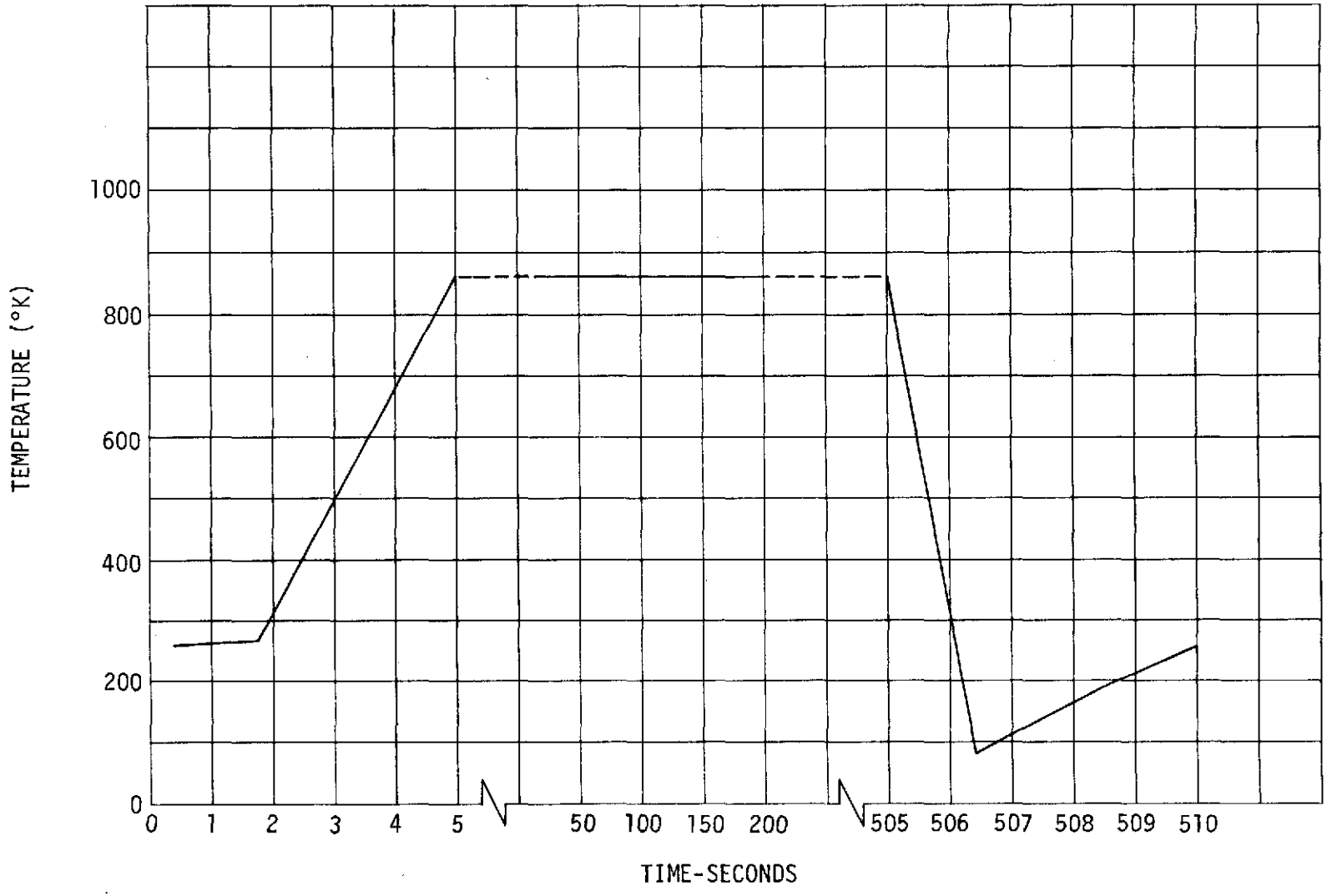

FIGURE 4.2-1: TEMPERATURE HISTORY FOR ELEMENT 7 (CYCLE 1,2,3)

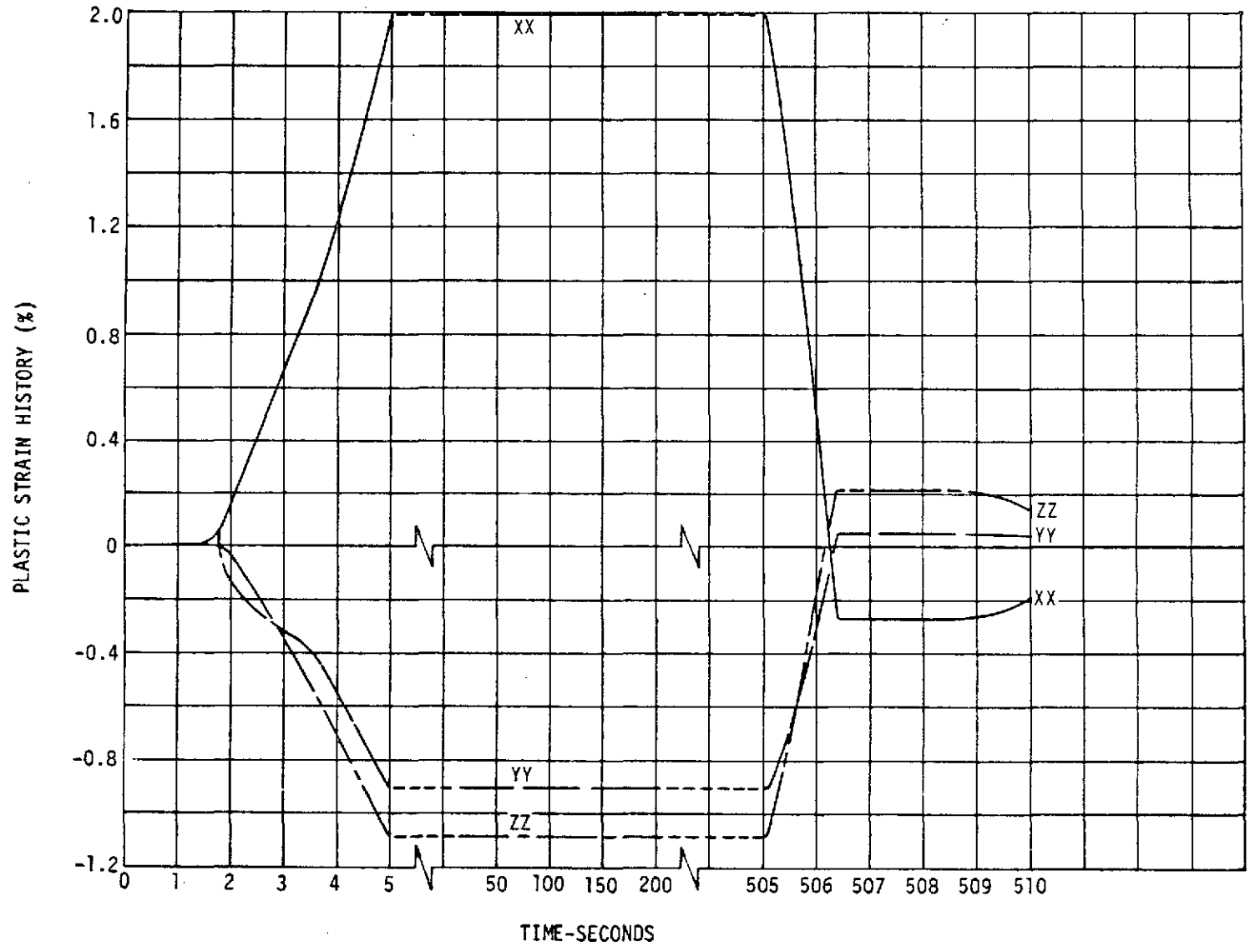

FIGURE 4.2-2: PLASTIC STRAIN HISTORY ELEMENT 7 (CYCLE 1)

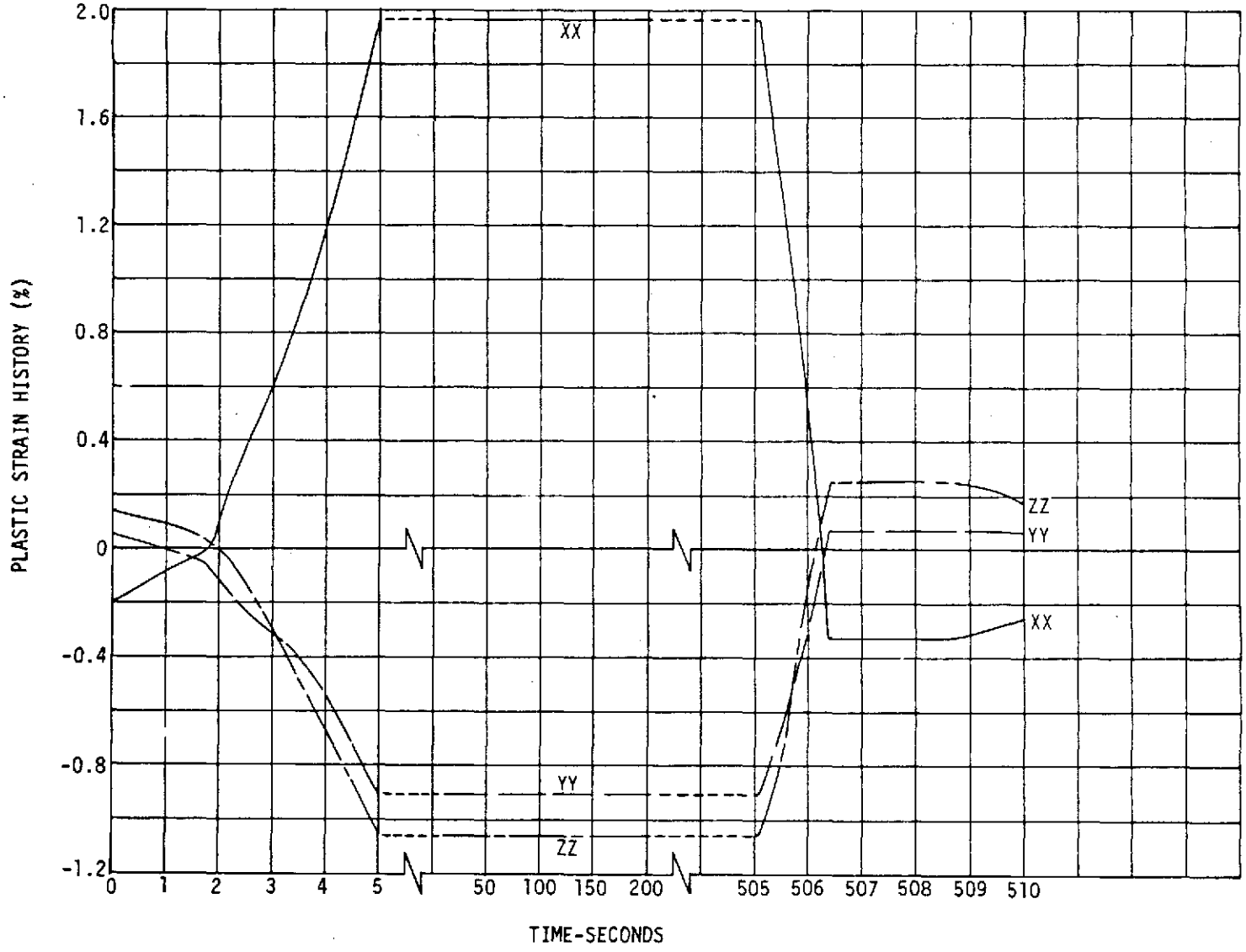

FIGURE 4.2-2 (CONT): PLASTIC STRAIN HISTORY ELEMENT 7 (CYCLE 2)

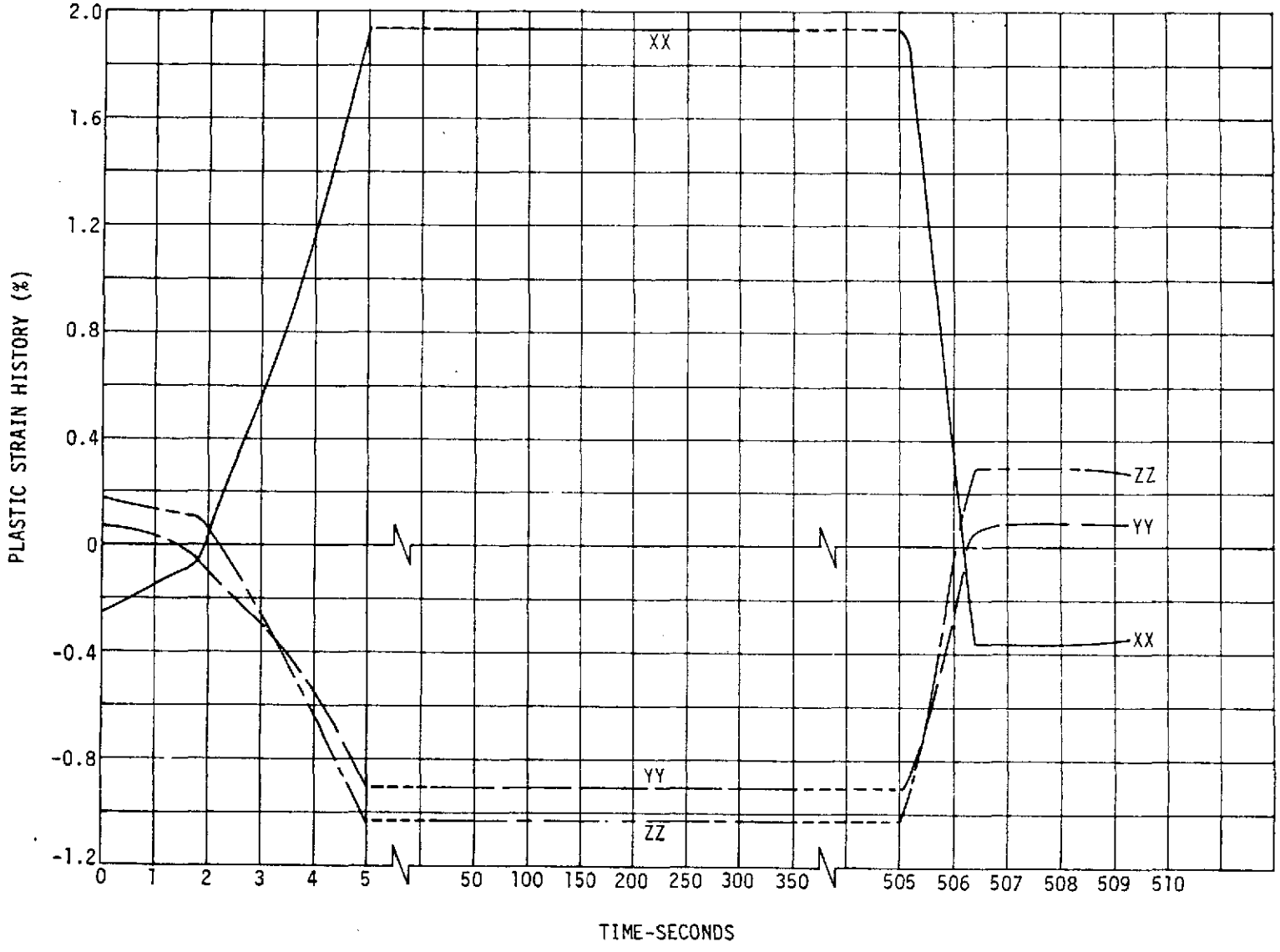

FIGURE 4.2-2 (CONT): PLASTIC STRAIN HISTORY ELEMENT 7 (CYCLE 3)

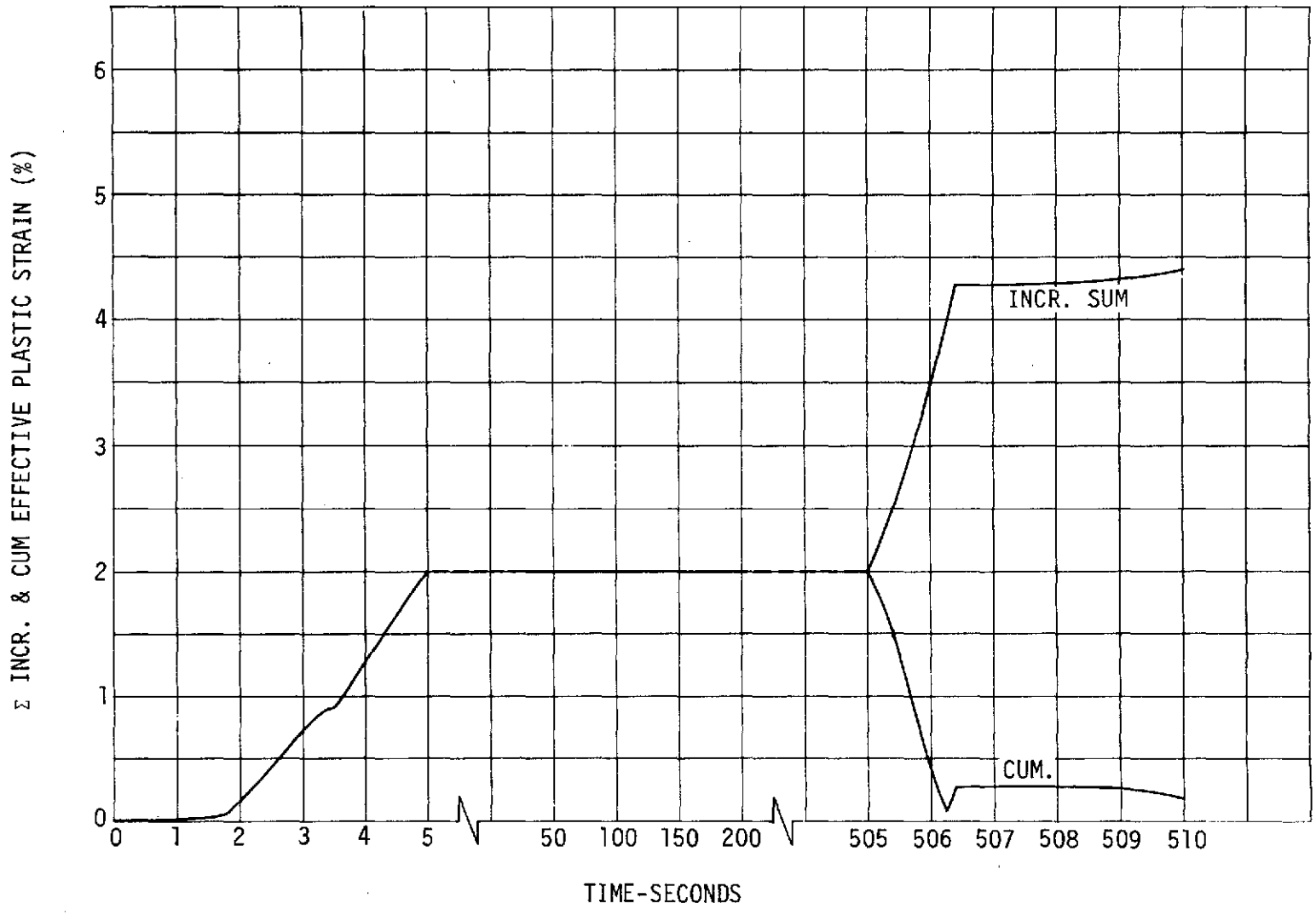

FIGURE 4.2-3: EFFECTIVE PLASTIC STRAIN AND INCREMENTAL SUM OF EFFECTIVE PLASTIC STRAIN FOR ELEMENT 7 (CYCLE 1)

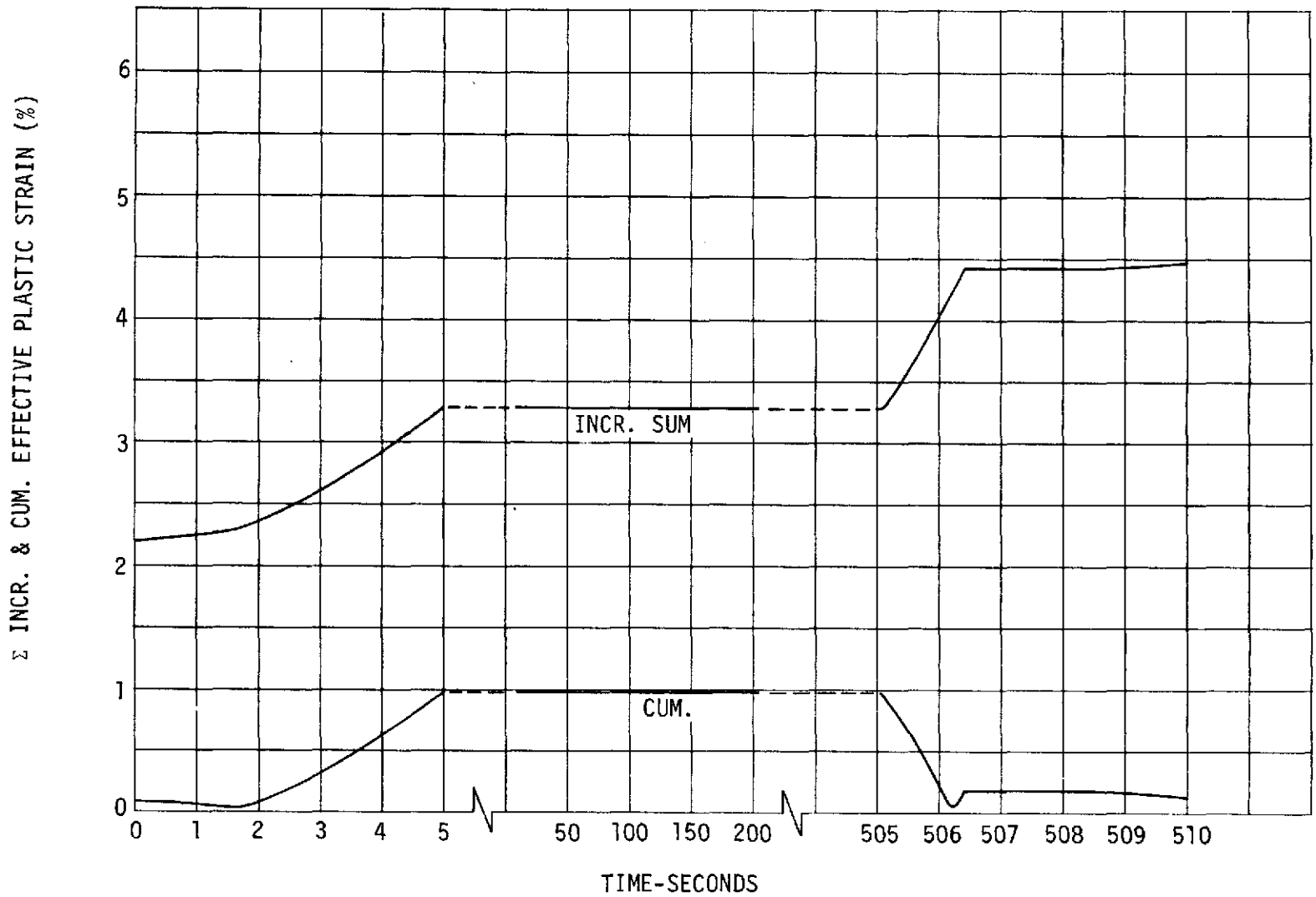

FIGURE 4.2-3 (CONT): EFFECTIVE PLASTIC STRAIN AND INCREMENTAL SUM OF EFFECTIVE PLASTIC STRAIN FOR ELEMENT 7 (CYCLE 2)

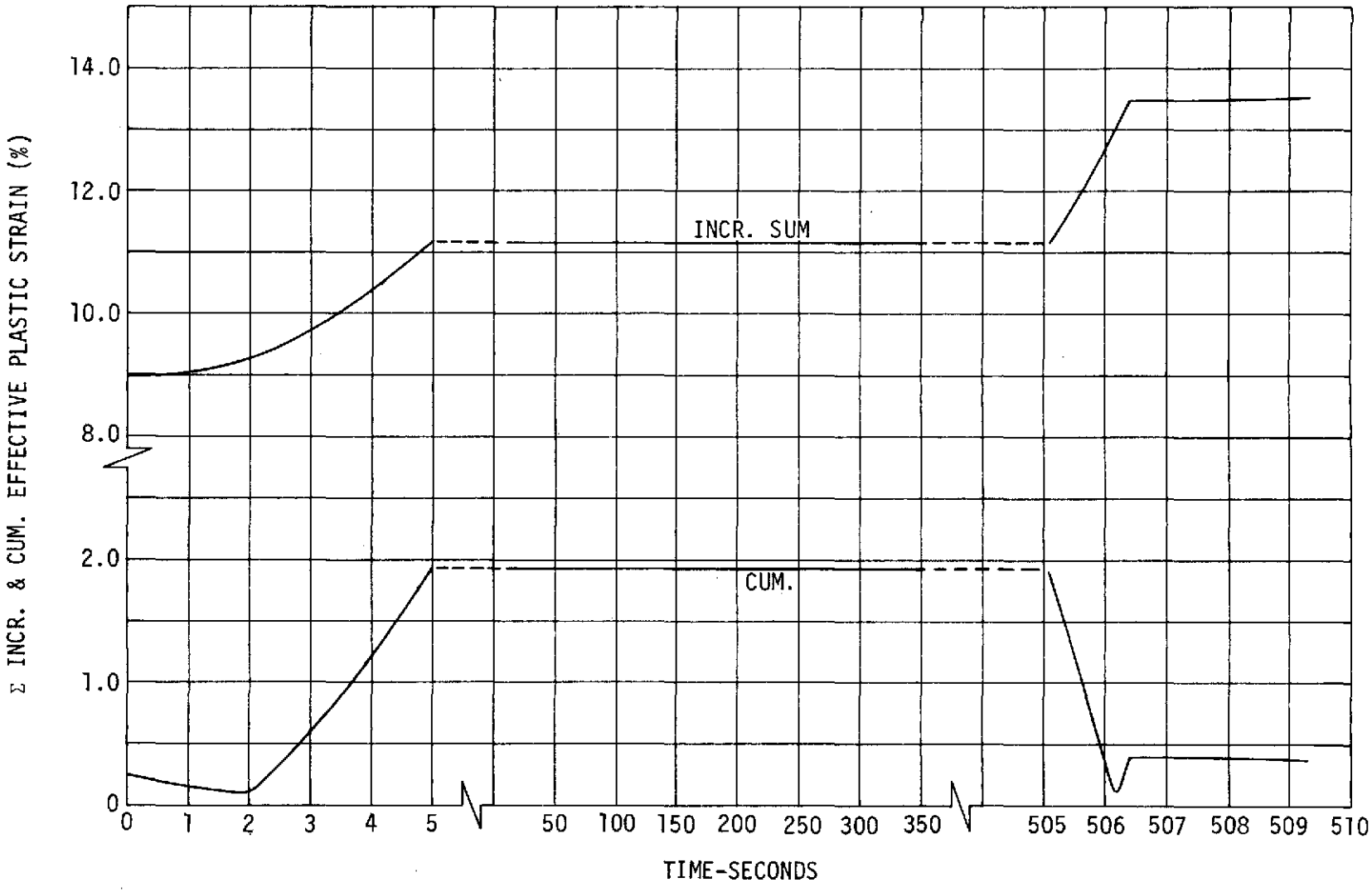

FIGURE 4.2-3 (CONT): EFFECTIVE PLASTIC STRAIN AND INCREMENTAL SUM OF EFFECTIVE PLASTIC STRAIN FOR ELEMENT 7 (CYCLE 3)

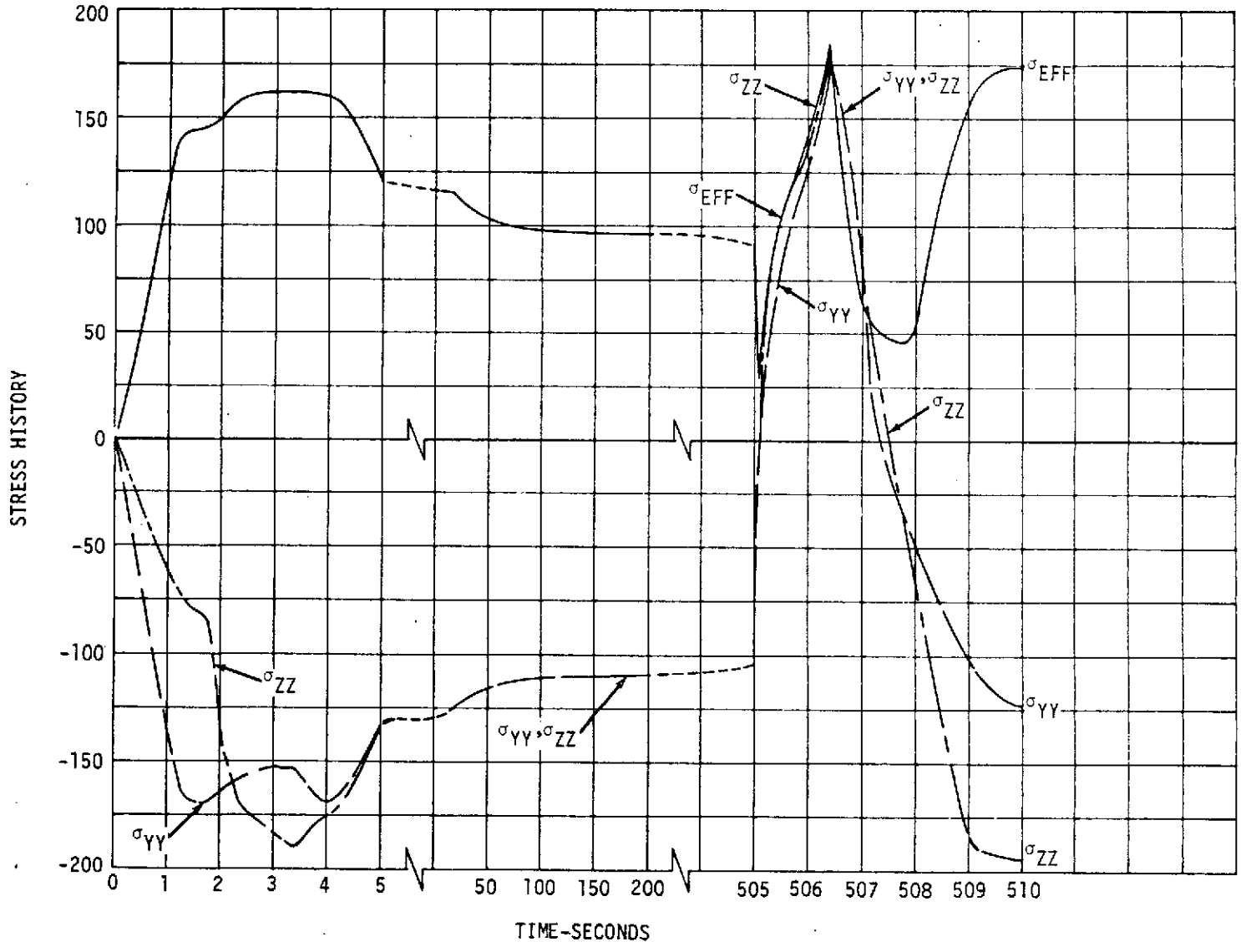

FIGURE 4.2-4: STRESS HISTORY FOR ELEMENT 7 (CYCLE 1)

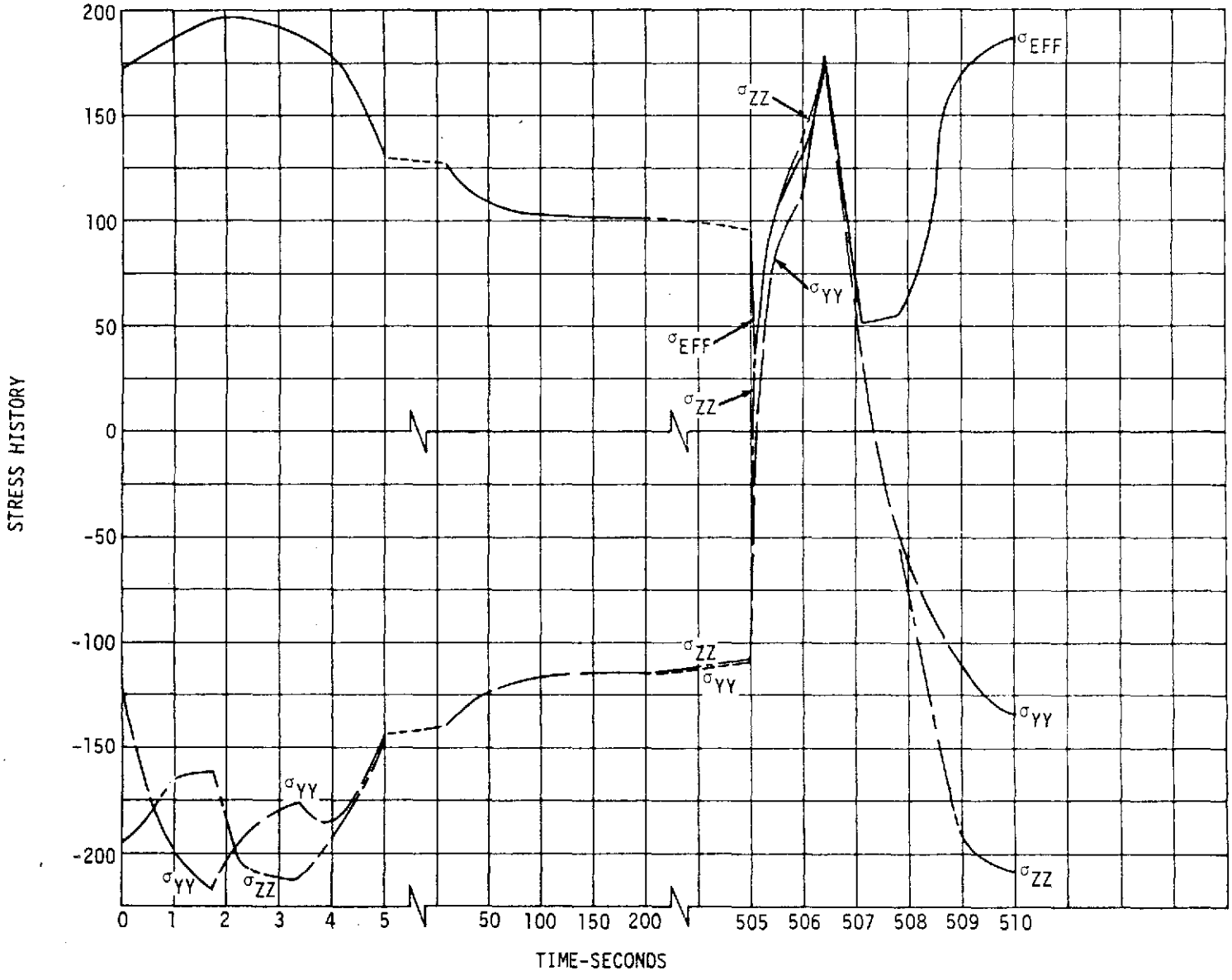

FIGURE 4.2-4 (CONT): STRESS HISTORY FOR ELEMENT 7 (CYCLE 2)

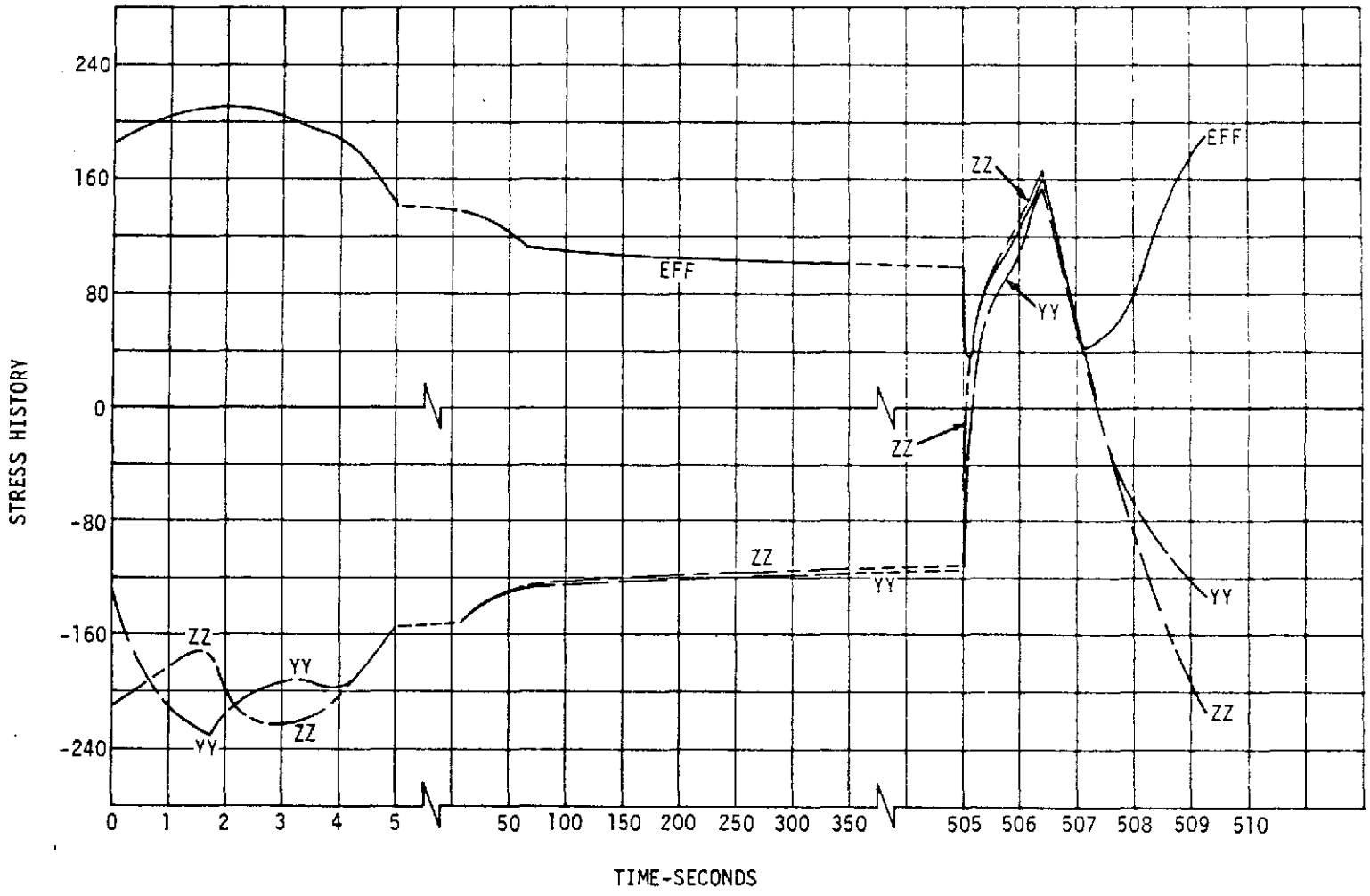

FIGURE 4.2-4 (CONT): STRESS HISTORY FOR ELEMENT 7 (CYCLE 3)

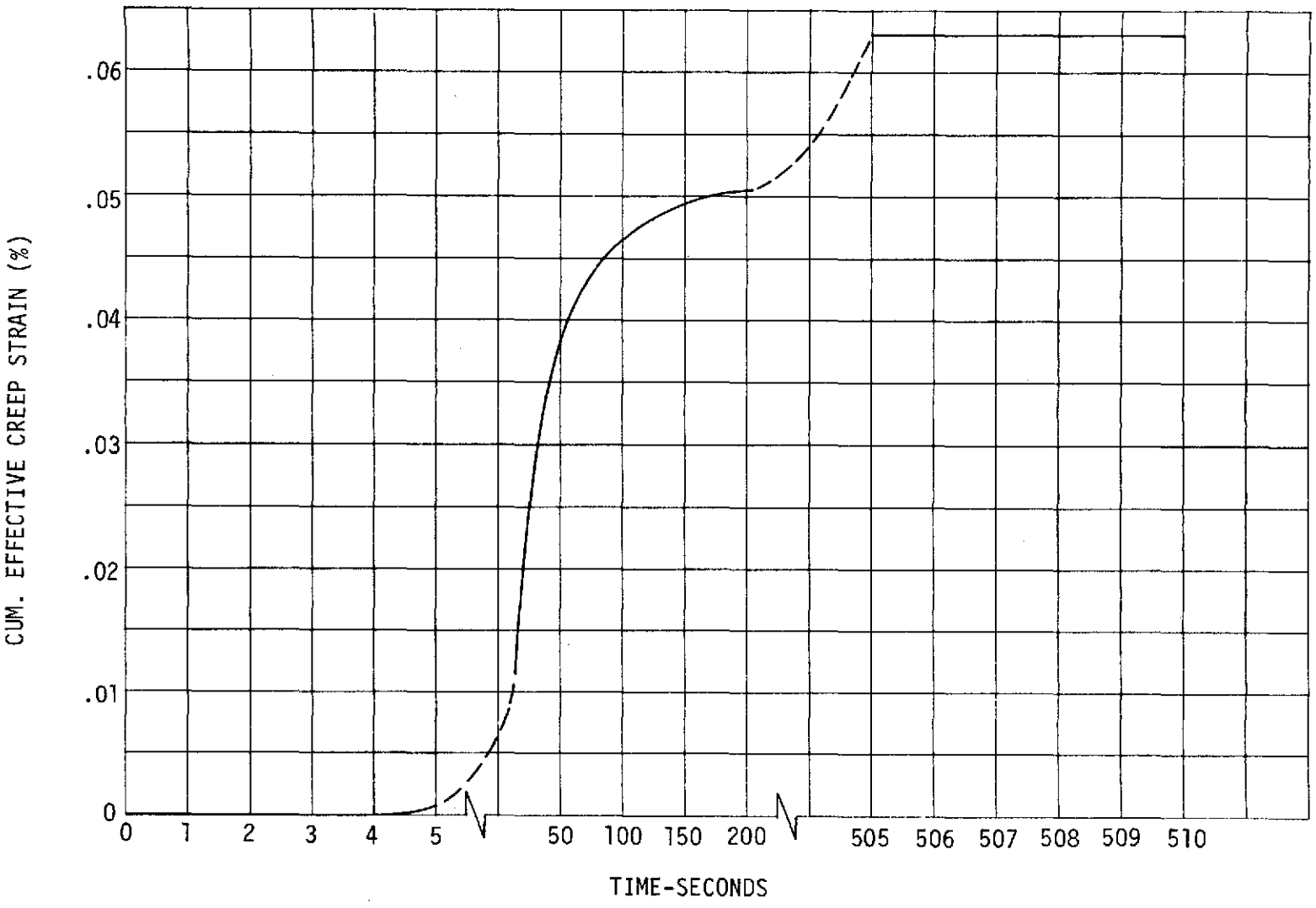

FIGURE 4.2-5: EFFECTIVE CREEP STRAIN HISTORY FOR ELEMENT 7 (CYCLE 1)

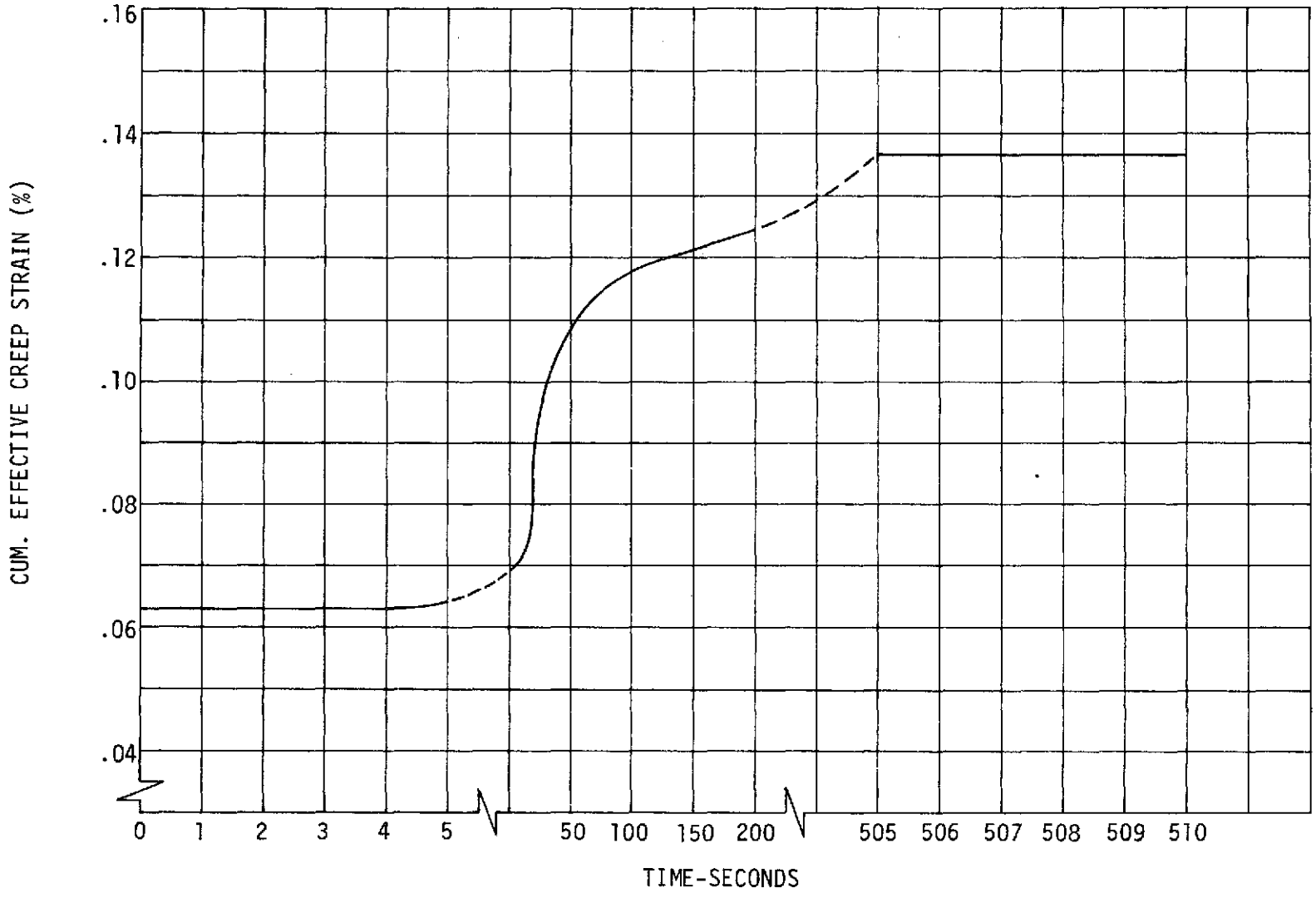

FIGURE 4.2-5 (CONT): EFFECTIVE CREEP STRAIN HISTORY FOR ELEMENT 7 (CYCLE 2)

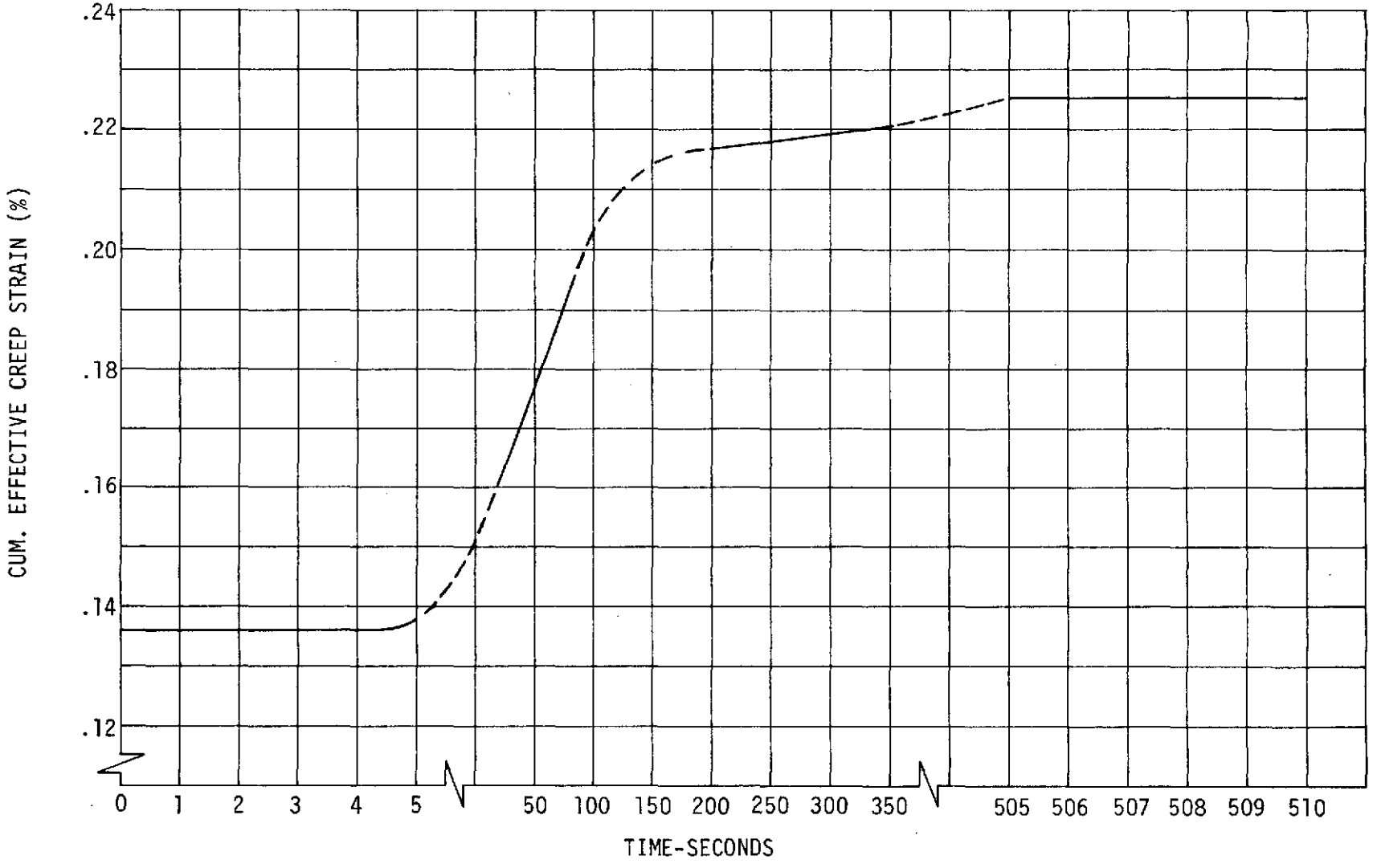

FIGURE 4.2-5 (CONT): EFFECTIVE CREEP STRAIN HISTORY FOR ELEMENT 7 (CYCLE 3)

THIS PAGE LEFT BLANK INTENTIONALLY.

5.0 CONCLUSIONS

For demonstration purposes, the analysis provided some guidelines for BOPACE analysis of the SSME engine:

(1) For the boundary conditions and material properties used in the analysis, temperature increments of about 39°K (70°F) produced good convergence for all increments. (Approximately 50 increments were required for each cycle.)

(2) Some experimentation was required to determine the proper creep time increments for the 500 second hold. Creep time increments which maintain effective creep strain increments less than about .01% produced good convergence.

(3) Even though the finite element model used was fairly coarse, it does provide good resolution of stress and strains in the important area near the hot gas wall. Some refinement of the model is desirable at the radius of the coolant channel, but otherwise, the model is adequate for further thrust chamber analysis. Approximately 3.8 hours of "task" time (IBM 360) were required to perform the thermal analysis, thermal data interpolation, model development, and execution of the three cycles.

The results of the analysis reveal three important aspects of the thrust chamber response to EPL operating conditions:

5.0 (Continued)

(1) As in previous analysis, the largest plastic strains occur at the hot gas wall at the centerline of the land area. The maximum effective plastic strain occurred at element 7. For the first cycle, the value was 2.0%; for the second cycle it decreased slightly to 1.97% and again to 1.93% for the third cycle.

(2) Creep strain which has not been included in any previous analysis of the SSME thrust chamber was found to accumulate from cycle to cycle although the magnitude of the creep strains were much smaller than the plastic strains. For element 7, the cumulative effective creep strain increased from .063% at the end of the first cycle to .136% at the end of the second cycle to .225% at the end of the third cycle. In light of the limited creep data available when the analysis was performed, the magnitudes of the creep strains may not be precise, but the cumulative behavior is indicative of the effects of the assumed engine cycle.

(3) The residual strains at the end of the cycle exhibit a behavior which has not been recognized in previous analysis. Figures 4.1-11, 4.1-15 and 4.1-19 show the trend of the residual plastic strains for the three cycles. A marked increase is shown particularly in the area near the coolant side wall. For example, the effective plastic strains for element 66

5.0 (Continued)

increase from .58% at the end of the first cycle to .84% at the end of the second cycle to 1.08% at the end of the third cycle. This indicates a possible "ratchet" behavior which may lead to larger plastic strains than predicted in previous single cycle analyses.

THIS PAGE LEFT BLANK INTENTIONALLY.

6.0 RECOMMENDATIONS

Based on the demonstration analysis, recommendations can be made for additional material test requirements and for additional analysis.

6.1 MATERIAL TEST REQUIREMENTS FOR BOPACE INPUT

In the demonstration analysis, only the cyclic behavior of the NARLOY-Z liner material was not determined from available experimental data. Experimental determination of strain-controlled hysteresis loops for NARLOY-Z for various temperatures and strain ranges would complete the material data package required for BOPACE analysis of the SSME thrust chamber liner.

6.2 FURTHER ANALYSIS

For further analysis, consideration should be given to the following:

(1) The finite element model used in the demonstration analysis (or even a simpler one) should be used for any further multiple cycle analysis to keep computation time to a minimum.

(2) Incorporation of the latest Boeing creep data for NARLOY-Z (Reference 9).

(3) Incorporation of a better representation of NARLOY-Z cyclic behavior as it becomes available.

(4) Incorporation of refinements to thermal and mechanical boundary conditions as they become available.

THIS PAGE LEFT BLANK INTENTIONALLY.

7.0 REFERENCES

1. "SSME Thrust Chamber - Preliminary Analysis of Temperature Transients Accompanying Engine Shutdown," Rocketdyne Internal Letter No. PAM 2112-2029 dated 12 July 1972.

2. "SSME Nominal Start Transient," Rocketdyne Internal Letter SSME 72-442 3112-3014, dated 1 March 1973.

3. "SSME Start to EPL," Rocketdyne Internal Letter SSME 73-1157 3112-3045, dated 9 May 1973.

4. "MCC Liner Finite Element Computer Run," Preliminary Copy of Rocketdyne Stress Analysis by L. B. Hocking dated December 4, 1972, and Number SSE 44-03-017.

5. "Material Properties Manual," Rocketdyne, Canoga Park, California.

6. R. G. Vos and W. H. Armstrong, "Improved Hardening Theory for Cyclic Plasticity," Technical Note, AIAA Journal, March 1973.

7. "Report on Preliminary NARLOY-Z Creep Tests," prepared by R. G. Vos, Boeing Structures and Propulsion Organization, 28 February 1973

8. Satoaki Omari, Klaus W. Gross and Alfred Krebsbach, "Wall Temperature Distirbution Calculation for a Rocket Nozzle Contour," NASA TN-D-6825, July 1972.

9. "NARLOY-Z Creep Test Report," prepared by D. C. Jerome, Boeing Structures and Propulsion Organization, 9 July 1973.

10. "Preliminary SSME Nozzle Throat Structural Temperatures," Boeing Memo 5-9432-H-059 dated 10 August 1972.

11. "Thermal Interpolation Computer Program," prepared by A. H. Spring, Boeing Structures and Propulsion Organization, March 13, 1973.

THIS PAGE LEFT BLANK INTENTIONALLY.